This is an *Accepted Manuscript*, which has been through the Royal Society of Chemistry peer review process and has been accepted for publication.

*Accepted Manuscripts* are published online shortly after acceptance, before technical editing, formatting and proof reading. Using this free service, authors can make their results available to the community, in citable form, before we publish the edited article. We will replace this *Accepted Manuscript* with the edited and formatted *Advance Article* as soon as it is available.

You can find more information about *Accepted Manuscripts* in the **Information for Authors**.

Please note that technical editing may introduce minor changes to the text and/or graphics, which may alter content. The journal's standard **Terms & Conditions** and the **Ethical guidelines** still apply. In no event shall the Royal Society of Chemistry be held responsible for any errors or omissions in this *Accepted Manuscript* or any consequences arising from the use of any information it contains.

# Mono- and Tri-Ester Hydrogenolysis using Tandem Catalysis. Scope and Mechanism[†]

Tracy L. Lohr,[a] Zhi Li,[a,d] Rajeev S. Assary,[b] Larry A. Curtiss,[b,c] Tobin J. Marks[a]*

[a] Department of Chemistry, Northwestern University, 2145 Sheridan Road, Evanston, IL 60208, USA.

[b] Materials Science Division, Argonne National Laboratory, Argonne, IL, USA, 60439

[c] Center for Nanoscale Materials, Argonne National Laboratory, Argonne, IL, USA, 60439

[d] Currently at: ShanghaiTech University, 100 Haike Road, Pudong District, Shanghai, China, 201210.

* Correspondence to: t-marks@northwestern.edu

**ABSTRACT.** The scope and mechanism of thermodynamically leveraged ester RC(O)O-R' bond hydrogenolysis by tandem metal triflate + supported Pd catalysts are investigated both experimentally and theoretically by DFT and energy span analysis. This catalytic system has a broad scope, with relative cleavage rates scaling as, tertiary >secondary >primary ester at 1 bar $H_2$, yielding alkanes and carboxylic acids with high conversion and selectivity. Benzylic and allylic esters display the highest activity. The rate law is $v = k[M(OTf)_n]^1[ester]^0[H_2]^0$ with an H/D kinetic isotope effect = 6.5 ± 0.5, implying turnover-limiting C-H scission following C-O cleavage, in agreement with theory. Intermediate alkene products are then rapidly hydrogenated. Applying this approach with the very active $Hf(OTf)_4$ catalyst to bio-derived triglycerides affords near-quantitative yields of $C_3$ hydrocarbons rather than glycerol. From model substrates, it is found that RC(O)O-R' cleavage rates are very sensitive to steric congestion and metal triflate identity. For triglycerides, primary/external glyceryl $CH_2$-O cleavage predominates over

secondary/internal CH-O cleavage, with the latter favored by less acidic or smaller ionic radius metal triflates, raising the diester selectivity to as high as 48% with $Ce(OTf)_3$.

**Broader Context**

This article reports the hydrogenolytic conversion of biomass relevant-esters to alkanes and carboxylic acids with high selectivity. For triglyceride esters, the glyceryl $C_3$ backbone is converted to alkanes (rather than undesirable glycerol) and useful oxygenates such as fatty acids, which can then be converted in-situ into biodiesel fuel. Produced from renewable or recycled biofeedstocks, biodiesel is playing an increasing role in the world's energy portfolio, meeting society's need for clean, sustainable energy. Biodiesel production currently relies on transesterification of naturally occurring fats or oils with simple alcohols such as methanol. This yields the corresponding fatty acid methyl esters (biodiesel), and large quantities of low-value glycerol by-product. The current economics of biodiesel depend critically on efficiently converting glycerol into valuable commodity chemicals, which has proven challenging. In contrast, we report a tandem catalytic system which completely bypasses glycerol to produce $C_3$ hydrocarbons together with mono and di-oxygenates. The latter are precursors to valuable 1,2- and 1,3-propane diols. Furthermore, waste oil fatty acid contaminants have no detrimental effects on this tandem catalyst. The versatility of this catalytic system offers promise for efficient biomass ether and ester C-O bond cleavage.

**Introduction**

The ester functional group is widely found in Nature, most commonly in the form of triglycerides (fats and oils), in both building blocks and chemicals from biomass degradation, as well as in many families of pharmacologically relevant natural products (e.g., Taxol drugs).[1, 2]

Esters are also extensively utilized in the pharmaceutical industry as protecting groups in synthesis, illustrating their versatility towards various chemical transformations.[3] Note also that esters are among the least reactive carbonyl functional groups (second to amides), which makes the development of selective and efficient cleavage methodologies highly desirable.[4] These issues are becoming increasingly relevant in the areas of sustainable biofeedstock processing[5-8] and polyester depolymerization/recycling for the mitigation of plastics environmental impact.[9]

Esters can undergo C-O cleavage via either $C_{acyl}$-O or $C_{alkoxy}$-O bond scission (Figure 1). While there are examples of ester cleavage by flash photolysis[10] and pyrolysis,[11] the more



**Figure 1.** Ester C-O cleavage pathways

common examples of $C_{acyl}$-O bond cleavage involve either acid-catalyzed hydrolysis[3, 12, 13] or oxidative addition to low-valent metal centers such as Ni(0),[14, 15] Rh(I),[16-18] Pd(0),[19-21] or Fe (II).[22, 23] Cleavage at the alkoxy juncture is by far the most common pathway for ester C-O bond scission applied to synthesis (Figure 2), and the majority of literature examples involve oxidative addition of conjugated (aryl, benzyl, allyl) C-O bonds to low-valent metal centers, which are subsequently applied in cross-coupling reactions with organoborane (Figure 2), organozinc, or Grignard reagents. The earliest examples (pre-2000) involve allylic ester C-O bond cleavage by oxidative addition to lower valent Co,[24] Ru,[24-28] Os,[26, 29] Pd,[19, 30] and Pt.[4] Photochemical oxidative addition to low-valent Mo has also been reported by Yamashita and co-workers.[31]

The move towards less expensive first row transition metals has seen the recent emergence of Ni-catalyzed $C_{aryl}$-O ester activations, with coupling to aryl boronic reagents the most heavily studied (Figure 2).[15, 32-35] However, reactions with organozinc reagents have also been

demonstrated to afford a wide variety of coupled products, while Li and co-workers reported Fe-catalyzed $C_{aryl}$-O cleavage in conjunction with electrophilic Grignard reagents. Recent reports from the Goldman[36] and Kakiuchi[37] groups provide examples of ester C-O bond cleavage
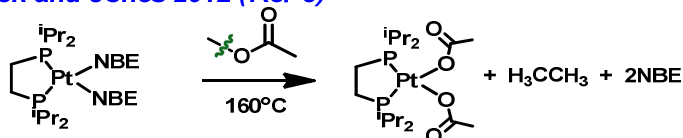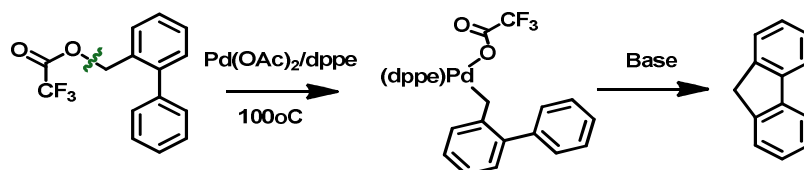


*Srivistava 1993 (Ref 13)*
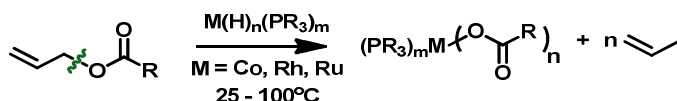
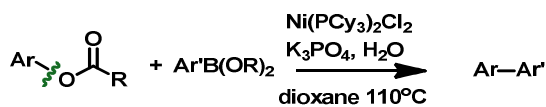*Planas and Komiya 2000 (Ref 14a)*
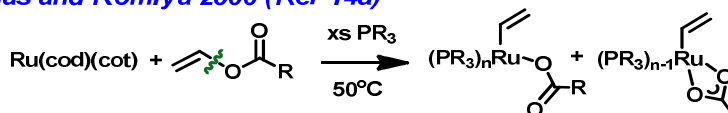
*Manbeck and Jones 2012 (Ref 3)*

*Hirano and Komine 2014 (Ref 16)*

*Example of Ni-catalyzed Caryl-O bond cleavage (Ref 9)*
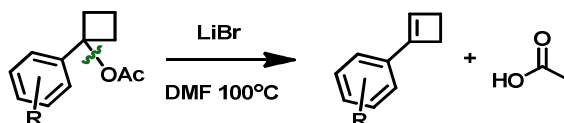
*Juteau and Gareau 1998 (Ref 21)*

**Figure 2**. Examples of alkoxy C-O bond cleavage. COD = 1,5-cyclooctadiene, COT: cyclooctatetrane, NBE = norborene, DPPE= 1,2-*bis*(diphenylphosphino)ethane.

following initial C-H activation at Ir and Ru, respectively. Goldman and co-workers also reported a (PCP)Ir pincer complex which reacts with methyl acetate via initial C-H activation at the carboxymethyl group to yield (PCP)Ir(H)(CH$_2$OAc), which subsequently undergoes ester C-O bond cleavage via carboxylate migration to produce the corresponding methyl acetate complex,

$(PCP)Ir(CH_3)(OAc).$[36] Ogiwara and Kakiuchi have reported overall C-H alkenylation with Ru that occurs via coordination of an allyl ester to yield a Ru-olefin complex that undergoes β-acetoxy elimination to form a Ru-acetate.[37]

Remarkably, Juteau and Gareau of Merck Frosst showed that transition metals are not always required to effect the cleavage of ester $C_{alkoxy}$-O bonds (Figure 2).[38] Under mild, neutral conditions, benzylic cyclobutyl acetates can be cleaved with LiBr to form the corresponding aryl cyclobutenes in good yields (50-97%). Very polar solvents such as DMF with addition of 10 - 20 eq of LiBr and heating to 140 °C required for optimum results. Electron-donating aromatic substituents increase the turnover rate while steric effects are minimal with substituents in the aryl ortho position.[38]

A common theme in the vast majority of transition metal or main group cation-mediated ester $C_{alkoxy}$-O bond cleavages is the requirement that the cleaved alkoxy group be either $sp^2$ hybridized, or $sp^3$ hybridized in conjugation with an allylic or benzylic π system. There are some reports of ester $C_{alkoxy}$-O cleavage with non-conjugated aliphatic substituents, however they involve forcing 250 - 500 °C decarboxylation with heterogeneous group 8 catalysts such as Pt,[39] Pd,[8, 40, 41] and Ni,[5, 7, 42-48] or 400 - 500 °C cracking over zeolites or $Al_2O_3$, to afford $CO_2$ and the corresponding hydrocarbons.[49-55] In summary, there is a current paucity of methodologies for aliphatic ester $C_{alkoxy}$-O bond cleavage under mild conditions without sacrificial carboxylic acid conversion to $CO_2$.

As noted above, esters are most commonly found in trigycerides (fats, oils) and are a promising source of renewable biodiesel fuel. Biodiesel has gained growing attention as an alternative to traditional diesel feedstocks, can be used directly in compression ignition engines without further engine modifications, and has the potential to supply a large portion of North

America's and Europe's energy market if obtainable from renewable resources.[6, 23, 56] Biodiesel is currently produced via the transesterification of triglycerides (animal and plant fats) with methanol to form fatty acid methyl esters (FAME's), defined as biodiesel, together with glycerol as a low value byproduct (see Scheme 1A below).[54, 57-61] The growing biodiesel enterprise has resulted in saturation of the glycerol market (> 1 million tonnes/year), where production has far
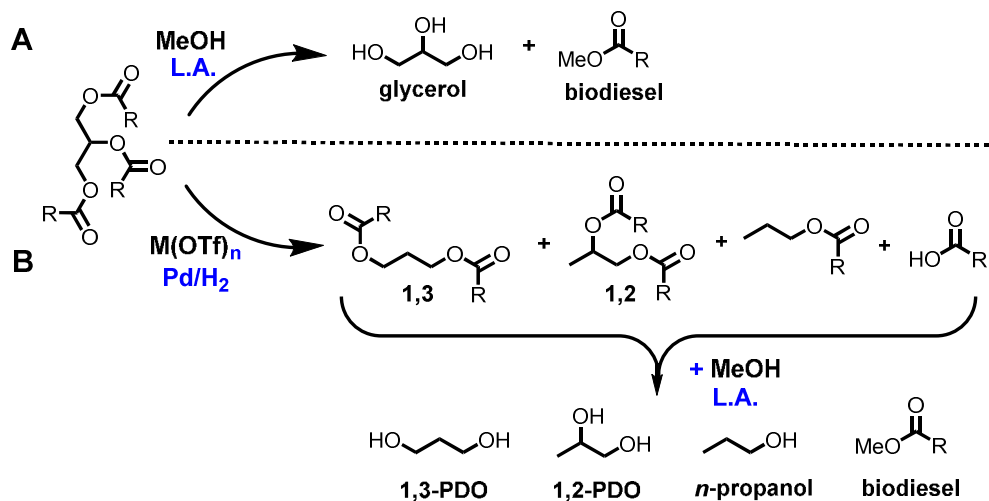


**Scheme 1**. Triglyceride C-O bond cleavage. **A**. Traditional transesterification route to produce glycerol and biodiesel. **B**. "Detoured" pathway that bypasses glycerol formation en route to biodiesel. L.A. = Lewis acid.

outpaced demand.[62-64] Thus, interest in glycerol valorization to commodity chemicals has recently resurged with the goal of enhancing the overall economic viability of biodiesel.[64-79] Furthermore, transitioning from traditional feedstocks such as edible plant and vegetable oils towards non-traditional ones such as waste oil, non-edible plant oil, and microalgae oil will be required to render future biodiesel production socially and economically responsible.[6] A major hurdle that accompanies transitioning to non-edible oil sources is free fatty acid (FFA) contamination, which forms soap in traditional base-catalyzed biodiesel synthesis, depresses catalytic rates, and adds extra purification/separation steps. A synthetic protocol that produces

biodiesel in the presence of FFA, without sacrificial loss in activity, would be highly desirable to further expand the renewable biodiesel enterprise.

Intense efforts are currently underway to valorize glycerol into commodity products such as 1,2-propanediol (1,2-PDO),[71, 80] 1,3-propanediol (1,3-PDO),[64] acrolein,[81] hydrogen,[82] and olefins.[70] Of these, 1,3-PDO is the highest value valorization product as a co-monomer for polypropylene terephthalate (PPT) production, as well as being used in a wide variety of cosmetics and lubricants.[64, 71] Note that 1,2-PDO is also used as a monomer for polyester resins, and as an antifreeze additive and paint component.[64, 83] Nevertheless, the selective valorization of glycerol to either 1,2-PDO or 1,3-PDO presents a "grand challenge," since the various conceivable intermediates undergo a multitude of undesired side reactions such as dehydration to ethers,[73] dehydrogenation to carbonyl-containing compounds, and retro-aldol processes.[78]

To address the aforementioned challenges associated with downstream glycerol valorization in biodiesel production, we sought to detour glycerol formation at an earlier stage in the biodiesel process (e.g., Scheme 1B). This "detoured" strategy could in principal generate 1,2-PDO, 1,3-PDO, 1-propanol, and possibly propane directly from the triglyceride $C_3$ backbone. This would require the clean selective cleavage of the triglyceride ester $C_{alkoxy}$-O bonds. We previously described the clean, efficient, and selective cleavage of etheric C-O bonds by a tandem metal triflate/supported hydrogenation catalyst system,[84-86] and recently communicated preliminary results showing that this catalytic system can also cleave ester $C_{alkoxy}$-O linkages (Figure 3).[87] Here we present a full discussion of our ester $C_{alkoxy}$-O hydrogenolysis studies, including a full mechanistic and theoretical investigation to define those factors governing the activity and selectivity of this tandem catalytic process. We also present a full account of triglyceride conversion by these tandem catalysts, including product selectivities and yields as a function of

conversion for multiple metal triflates, different metal triflate : Pd ratios, and optimization of reaction conditions.

**Experimental Section**

**Materials and methods**. Anhydrous grade substrates were obtained from commercial vendors and used as received unless otherwise noted. Commercially unavailable substrates, reaction intermediates and products, were independently synthesized by esterification of corresponding alcohol with requisite acyl chloride or anhydride, mediated by triethylamine and *N,N*-dimethylamino pyridine (DMAP), according to literature procedures.[87] Anhydrous organic solvents and Pd catalysts were obtained from commercial vendors and used as received. The hydrogenation catalyst, 5% Pd on $TiO_2$ (Degussa P25, surface area 50 $m^2$/g, dispersion 16.1 %) was prepared via literature proceduers[88] by wet impregnation with $Pd(OAc)_2$, calcined at 550 °C under $O_2$, and then reduced at 300 °C under 5% $H_2$ in $N_2$ before use. THF was dried by distillation from Na/benzophenone. Trifluoro-methanesulfonic acid was obtained from Sigma-Aldrich and purified by vacuum distillation before use. Metal triflates were obtained from commercial vendors and dried by heating to 100 °C under high vacuum before use. $Zr(OTf)_4$ was synthesized according to previously reported procedures,[89] and tricaprylin was purchased from Sigma Aldrich and dried over molecular sieves before use. Cyclohexanone-2,2,6,6-$d_4$ was purchased from Santa Cruz Biotechnology and used as received.

All manipulations of reagents were carried out in oven-dried reaction vessels unless otherwise noted. Reactions of mono-esters under 1 bar $H_2$ atmosphere were carried out in cylindrical reactors equipped with rubber septa, a magnetic stirbar, and an $H_2$ balloon, with heating supplied by an oil bath. Reactions of triglycerides under 1 bar $H_2$ atmosphere (Table S3) were carried out in a glass reactor sealed with ground glass stopper having a gas inlet. Reactions

of triglycerides under higher pressure were performed in a 10 mL HEL or 100mL Parr reactor (Model 4590, Parr Company, Moline, IL) equipped with mechanical stirring within a Teflon liner, capable of reaching a maximum temperature of 300°C, maximum pressure of 750 psi (50 bar), and maximum stirring rate of 3000 rpm. Esters were either purchased from commercial vendors or synthesized according to previously published procedures as noted above.[87]

**Physical and Analytical Measurements.** Thin-layer chromatography (TLC) was performed on EMD Millipore pre-coated TLC plates (silica gel 60 GF254, 0.25 mm). Flash chromatography and filtration through silica were performed on flash grade silica gel (32-63u) from Dynamic Adsorbents Inc., GA. NMR spectra were recorded on a Varian Inova-500 (FT, 500 MHz, $^1$H, 100 MHz, $^{13}$C), a Varian Inova-400 (FT, 400 MHz, $^1$H, 100 MHz, $^{13}$C, 376 MHz, $^{19}$F) or a Mercury-400 (FT, 400MHz, $^1$H; 100 MHz, $^{13}$C) spectrometer. Chemical shifts (δ) for $^1$H, and $^{13}$C are referenced to internal solvent. GC-MS analysis was performed on a Waters GCT Premier GC-TOF, coupled to an Agilent 7890A GC with a DB-5MS (5% phenyl methyl siloxane, 30 m × 250 μm × 0.25 μm) capillary column and a time-of-flight (TOF) high resolution detector. GC-TCD tests of gas samples were performed on a three-channel Agilent MicroGC system equipped with TCD detectors and molecular sieves, Plot U, and alumina columns for each channel. High resolution mass spectrometry was performed on an Agilent 6210A LC-TOF to obtain accurate molecular weight information.

**Synthesis of 2,2,6,6-$d_4$-Cyclohexanol.** A round bottom flask equipped with an $N_2$ inlet and a magnetic sir bar was charged with 2.0 g (53 mmol) of LiAlH$_4$ and 100 mL anhydrous diethyl ether. The flask was cooled in an ice-water bath. To the solution was slowly added 5.0 g (50 mmol) cyclohexanone-2,2,6,6-$d_4$ via syringe, which was then allowed to warm to room temperature with stirring overnight. The reaction was then quenched by adding 50 mL deionized

$H_2O$ to afford a white paste, which was dissolved, under vigorous stirring, with 50 mL aqueous 1.0 M HCl solution. The mixture was then extracted with 3 x 50 mL diethyl ether. The combined organic phase was washed sequentially with 50 mL each of saturated $NaHCO_3$ solution and an NaCl solution before drying over $Na_2SO_4$, filtering, and concentrating to afford 4.8 g product in 92% yield. The product was used in the next synthetic step without further purification. $^1$H NMR (400 MHz, $CDCl_3$): δ 3.59 (s, 1 H), 1.76-1.67 (m, 2 H), 1.61 (s, O*H*, 1 H), 1.58-1.49 (m, 1 H), 1.31-1.21 (m, 2 H), 1.21-1.10 (m, 1 H). $^{13}$C NMR (100 MHz, $CDCl_3$): δ 70.3, 35.6, 25.5, 24.1.

**General procedure for ester substrate synthesis**. A 500 mL round-bottom flask was charged 20 mmol (1.0 equiv) of alcohol, 1.5 equiv of triethylamine, 5 mol% of DMAP, and 50 mL $CH_2Cl_2$. To the resulting solution was added dropwise 1.5 equiv of acyl chloride or anhydride at 0°C with magnetic stirring. After addition, the reaction was brought to rt and stirred until the alcohol was consumed (as monitored by TLC). The reaction was then quenched by adding 60 mL of 1M HCl solution, and the organic layer was separated. To the organic layer was added 20 mL saturated $NaHCO_3$ solution and the biphasic mixture was stirred for 30 min at rt to remove excess acyl chloride or anhydride. The organic phase was then separated, washed sequentially with 2 x 25 mL saturated $NaHCO_3$ solution and 2 x 25 mL brine, and then dried over $Na_2SO_4$, filtered, and concentrated. The residue was passed through a 10x10 cm silica plug with 10:1 hexanes/ethyl acetate as the eluent. Evaporation of the collected fractions afforded desired ester products.

**2,2,6,6-*d_4*-Cyclohexyl acetate:** Yield 5.4g, 79%. $^1$H NMR (500 MHz, $CDCl_3$): δ 4.71 (s, 1 H), 2.03 (s, 3 H), 1.74-1.67 (m, 2 H), 1.58-1.50 (m, 1 H), 1.38-1.29 (m, 2 H), 1.28-1.18 (m, 1 H). $^{13}$C NMR (100 MHz, $CDCl_3$): δ 170.8, 72.7, 31.0 (m, *C*$D_2$), 25.4, 23.8, 21.6. LIFDI-MS: (M+) m/z Calculated: 146.1249. Found: 146.1307.

**Cyclohexyl benzoate**[90] was prepared using the aforementioned esterification procedure from the corresponding alcohol, and the NMR data agrees with the literature.

**General procedures for experiments performed at 1 bar $H_2$.** A 16 x 100mm test tube was charged with a magnetic stir bar, metal triflate, and hydrogenation catalyst (amounts subject to specific conditions), and then sealed with a rubber septum through which a balloon was attached. The test tube and balloon were carefully purged with gaseous $H_2$ three times, charged with $H_2$, and then heated in an oil bath at the desired reaction temperature for 30 min with stirring. The test tube was charged with 1.0 mmol of substrate via syringe and stirred at a rate of 700 rpm. Aliquots (0.1 mL) were syringed out at predetermined times for $^1$H-NMR analysis (in 0.4 mL of $CDCl_3$) from which conversion was determined by integration versus mesitylene internal standard. In cases of solvent screening experiments, a 1.0 M solution of substrate in the specified solvent was added.

**General procedures for 1 bar $H_2$ pressure triglyceride reactions**. To prevent gas permeation which might compromise the accuracy of gaseous product analysis, 1 bar reactions were performed in sealed glass tubes without a balloon. A 50 mL glass test tube with ground joint was charged metal triflate, 10% Pd/C (amounts subject to specific conditions), 1.0 mmol substrate (tricaprylin **5a**, tristearin **5b**, or glycerol), and a magnetic stir bar. A 250 mL solvent bulb equipped with a glass adapter with stopcock was fitted to the test tube and secured with clips, bringing the total gas volume to ~300 mL. The apparatus was next purged with vacuum/1 bar $H_2$ for 3 cycles, and the glass tube then brought to the reaction temperature in an oil bath (150 °C) or a sand bath (200 °C) with stirring at 700 rpm. After 2 h, the reaction was halted and the glass tube cooled to rt. Before opening the glass apparatus, GC-TCD analysis was first performed by connecting the adapter to the GC gas inlet. After the GC analysis, the apparatus was opened and

NMR analysis of the condensed phase was performed after adding a known amount of mesitylene as internal standard. "Carboxylate balance" of the RCOO moiety was determined by summing the calculated content of all RCOO-containing species (**6**, **7**, **8**, **9**, and **10**) versus that contained in the starting material (**5**).

**General procedures for high pressure triglyceride reactions**. A 100 mL Teflon liner was charged metal triflate, 10% Pd/C (amounts subject to specific conditions), and 14.0 mmol tricaprylin. The liner was then placed in the Parr reactor and sealed. The reactor was next purged 10x with 10 bar $H_2$ before being pressurized to the designated pressure and then brought to the reaction temperature with vigorous mechanical stirring. After 2 h, the reaction was halted and the reactor cooled to 25°C. Before opening the reactor, gas samples were collected through the vent port into a purged glass sampling bag and analyzed by GC-TCD. After opening the reactor, NMR analysis of the condensed phase was performed with an aliquot of resulting mixture, using the terminal methyl shift ($\delta$ 0.92-0.85) as an internal standard since it remains unchanged throughout the reaction. Control experiments also show that the coke formation is minimal (<1%). The RCOO moiety "carboxylate balance" was determined by summing the content of all RCOO-containing species (**6**, **7**, **8**, **9**, **10**) versus that contained in the starting material (**5**).

**Analysis of cyclohexyl acetate conversion as a function of reaction temperature.** Runs were performed in 16 x 100mm test tubes with a magnetic stirring bar and a $H_2$ balloon under the conditions for conducting reactions at 1 bar $H_2$ described above. The stirring rate was set at 800 rpm. For kinetic analysis, a stock solution was prepared consisting of cyclohexyl acetate (10 mL, 68 mmol, 92% V/V), Hf(OTf)$_4$ (0.2632g, 0.5 mol%), and mesitylene (1mL, 7 mmol). Pd/C (11.9 mg, 0.2 mol%) was added to the test tube and the system purged with $H_2$ 3x. The test tube was then placed in an oil bath at the appropriate temperature for 30 min to ensure that the Pd/C was

fully reduced. The stock solution of cyclohexyl acetate, $Hf(OTf)_4$, and mesitylene (0.9 mL) was briefly sonicated to ensure the $Hf(OTf)_4$ was dissolved before addition via syringe. Aliquots (0.05 mL) were removed from the condensed phase at predetermined times and added to $CDCl_3$ (0.4 mL) for $^1H$ NMR analysis. Conversion was determined by integration versus mesitylene.

**Cyclohexyl acetate conversion as a function of [Hf(OTf)$_4$].** Runs were performed in 16 x 100mm test tubes with a magnetic stirring bar and a $H_2$ balloon under the modified conditions for conducting reactions at 1 bar $H_2$ mentioned above, with stirring at 800 rpm. The appropriate amount of Pd/C was added to the test tube, followed by purging with $H_2$ for 3x times. The test tube was then placed into an oil bath at 100 °C for 30 min to allow the Pd/C to pre-reduce. A separate test tube was charged with the appropriate amount of $Hf(OTf)_4$ along with 1 mL cyclohexyl acetate and 0.05 mL mesitylene. This was briefly sonicated to completely dissolve the $Hf(OTf)_4$, and the solution added via syringe to the Pd/C under $H_2$ at 100 °C. Aliquots (0.05 mL) were taken from the condensed phase at preselected times and added to $CDCl_3$ (0.4 mL) for $^1H$ NMR analysis. Conversion was determined by integration versus the mesitylene standard. For all experiments at different [$Hf(OTf)_4$], the ratio between Hf and Pd was kept constant at 5:2.

**Cyclohexyl acetate conversion as a function of H$_2$ pressure.** Mesitylene was not used as an internal standard due to competing hydrogenation at higher pressures. A stock solution of cyclohexyl acetate (10 mL, 68 mmol), $Hf(OTf)_4$ (0.2632g, 0.5 mol%), and 1,1,2,2-tetrachloroethane (0.5 mL, 4.7 mmol) was prepared. The cyclohexyl acetate stock solution (0.25 mL) and Pd/C (3.4 mg, 0.2 mol%) were added to a HEL reactor with a magnetic stir bar. The system was purged with $H_2$ to 15 bar 5x before setting to the desired pressure. The reactor was heated to 100 °C for 1 h, stirring at 800 rpm, then cooled to 10 °C in an ice bath, opened, and a

0.05 mL aliquot withdrawn and added to $CDCl_3$ (0.4 mL) for $^1H$ NMR analysis of % conversion versus the internal standard, 1,1,2,2-tetrachloroethane.

**Kinetic isotope effect.** Two stock solutions were prepared with 2.0 mL of either cyclohexyl acetate or 2,2,6,6-$d_4$-cyclohexyl acetate plus $Al(OTf)_3$ (31.3 mg, 0.50 mol%). The appropriate stock solution (0.40 mL) was then added to the 10 mL HEL reactor along with Pd/C (0.0058g, 0.20 mol%), a magnetic stir bar, and either 2.0 mL of cyclohexane solvent or neat stock solution. The reactor was next pressurized to 40 bar $H_2$, and heated to 125 $^oC$ for 2.0 h (proteo substrate) or 6.0 h (deutero substrate), then cooled in an ice bath. Conversion was quantified by NMR from the ratio of the cyclohexyl acetate $CH_3$ signal to the AcOH $CH_3$ signal for the proteo and deutero substrates, respectively. The KIE value reported is an average of 8 trials (4 neat, and 4 with 2.0 mL cyclohexane).

**Computational Details**. All calculations were performed using Gaussian 09 software.[91] An unrestricted B3LYP density functional was employed for all energy and geometry evaluations.[84-86] The Stuttgart RSC 1997 ECP basis set was used for Hf atom and 6-31+G(d) basis set for rest of the atoms. All structures were optimized in the gas phase with no geometry constraints. Frequency calculations were performed to evaluate enthalpy and free energy corrections at 298 K. For transition state evaluations, frequency calculations were performed to confirm the transition states. Intrinsic reaction coordinate (IRC) calculations are also performed to confirm the existence of transition states.

To compute the energy landscape of the $Hf(OTf)_4$-catalyzed conversion of cyclohexyl acetate (ester) to cyclohexane in solution, the solvation contribution was included using a dielectric medium of 2-butanol (dielectric constant = 15.9) with the SMD solvation model via a single point energy calculation at the B3LYP level of theory with the same basis sets used in the

geometry optimizations. Such a treatment was previously found adequate in mapping the relative energetics in solution media for other C-O bond cleavages catalyzed by lanthanide triflates.[85, 86]

**Results**

The goal of this investigation is to explore the scope and mechanistic understanding of ester RC(O)O-R' hydrogenolysis catalyzed by a tandem metal triflate + supported hydrogenation catalyst system,[35] with particular focus on triglyceride reactivity. The effects of different metal triflates and hydrogenation catalysts on rates and selectivity are discussed first, along with solvent effects. Second, the effects of varying the carboxylate acyl group substituent and the ester alkoxy group on the reaction rates are explored. The reaction kinetics and mechanism are then evaluated on the basis of the rate laws, activation parameters, and kinetic isotope effects. Triglyceride reactivity along with an assessment of hydrogenolysis selectivity are then presented, followed by a DFT computational analysis of the reaction mechanism.

*1.1 Catalyst and Solvent Effects.* The effects of metal triflate ionic radius and other characteristics, as well as the hydrogenation catalyst identity were investigated using the model substrate cyclohexyl acetate (Figure 3 and Table S1). As can be seen in Figure 3 and as previously reported for ether hydrogenolysis,[84-86] metal triflates with higher calculated effective charge density ($p$) on the central metal ion are the most active Lewis acid catalysts. While most lanthanide triflates are inactive for 2° ester cleavage at 125 °C/1 bar $H_2$, $Ce(OTf)_3$, $Fe(OTf)_3$, and $Al(OTf)_3$ exhibit moderate activity, with the highest activity achieved using $Hf(OTf)_4$, which reaches conversions up to 89% after 1 hour at 125 °C (Figure 3). These experiments also reveal that reactions with HOTf as the acid catalyst are significantly less rapid (20% after 1 hour), arguing that metal triflate catalyzed RC(O)O-R' cleavage reactions do not, in most cases, depend

significantly on hydrolysis of the metal triflate to form HOTf.  A similar conclusion was reached

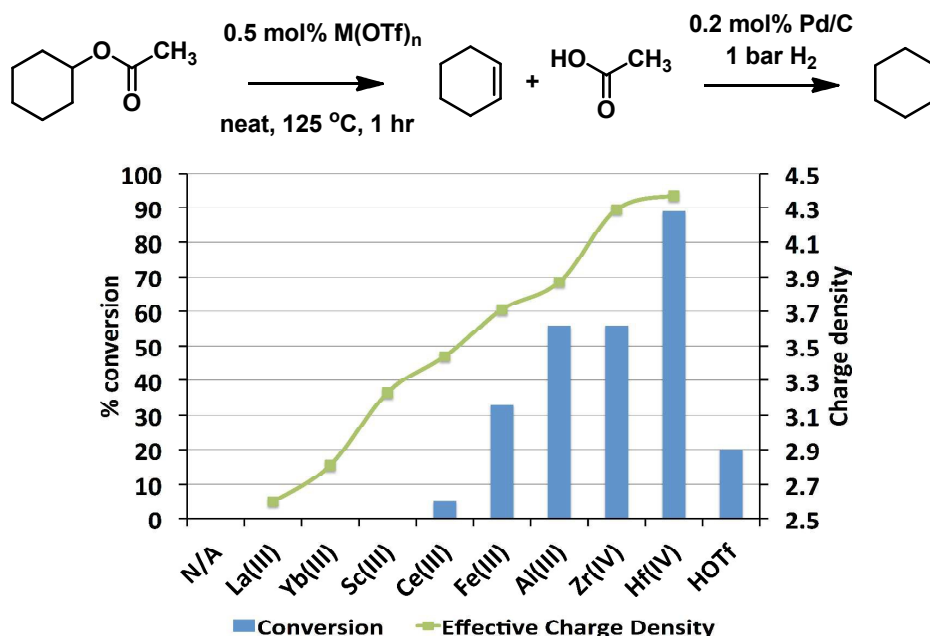for ether hydrogenolysis by a number of experiments/confirmatory tests.[84-86]



**Figure 3**. Plots of cyclohexyl acetate conversion as a function of metal triflate catalyst and comparison to DFT computed effective metal ion charge density.[84-87] Conditions: 0.5 mol % metal triflate, 0.2 mol% Pd/C (10 wt%), 125 °C, 1 bar $H_2$, neat substrate.

The effect of the heterogeneous Pd hydrogenation catalyst support on hydrogenolysis activity

was also surveyed. Using $Hf(OTf)_4$ as the Lewis acid catalyst, commercially purchased  Pd/C

and $Pd/SiO_2$ afford similar results, reaching 89 and 85% conversion, respectively, of cyclohexyl

acetate after 1 hour at 125 °C (Table S1). The yields fall slightly to 75% using $Pd/TiO_2$, and are

significantly depressed using commercially purchased $Pd/BaSO_4$ (15%) or $Pd/Al_2O_3$ (31%). This

is not entirely surprising since the Lewis basicity of the support[92] may inhibit the activity of the

Lewis acid catalyst through competitive binding to the support. Alternatively, changing the

support identity has been found previously to alter the hydrogenation activity of Pd catalysts, so

it is not surprising that $Pd/BaSO_4$ and $Pd/Al_2O_3$ exhibit lower rates of hydrogenation in this

system.[93-95]  Indeed, using $CeO_2$ as a support yields negligible cyclohexyl acetate conversion for

either Pd or Pt catalysts. Readers are directed to reference 95 for a more detailed discussion on Pt group hydrogenation catalysts.[95]  Choice of solvent, with corresponding dielectric constants ($\varepsilon$), also affects the rates of ester hydrogenolysis (Table S1). Thus, reaction media such as neat substrate, here cyclohexyl acetate ($\varepsilon = 5.08$), yields the highest activities versus $CHCl_3$ ($\varepsilon = 4.81$) and *n*-octane ($\varepsilon = 1.96$). Using more polar/Lewis basic solvents with higher dielectric constants such as THF ($\varepsilon = 7.58$), MeOH ($\varepsilon = 32.7$), DMF ($\varepsilon = 36.7$), or $H_2O$ ($\varepsilon = 80.1$) leads to negligible conversion, most likely due to Lewis acid catalyst poisoning, thus reconfirming the important role of the Lewis acid metal center in this tandem reaction. Cyclohexyl acetate is insoluble in $H_2O$, which could also be responsible for the observed lack of activity in that solvent.

*1.2 Acyl and Alkoxy Group Effects*. Substituent effects on the acyl and alkoxy group were also investigated (Figures 4 and 5). Sequentially replacing the methyl hydrogen atoms of cyclohexyl acetate with methyl groups (R = Me < Et < $^i$Pr < $^t$Bu; Figure 4, blue columns) monotonically depresses the turnover frequency (TOF), under identical reaction conditions, from
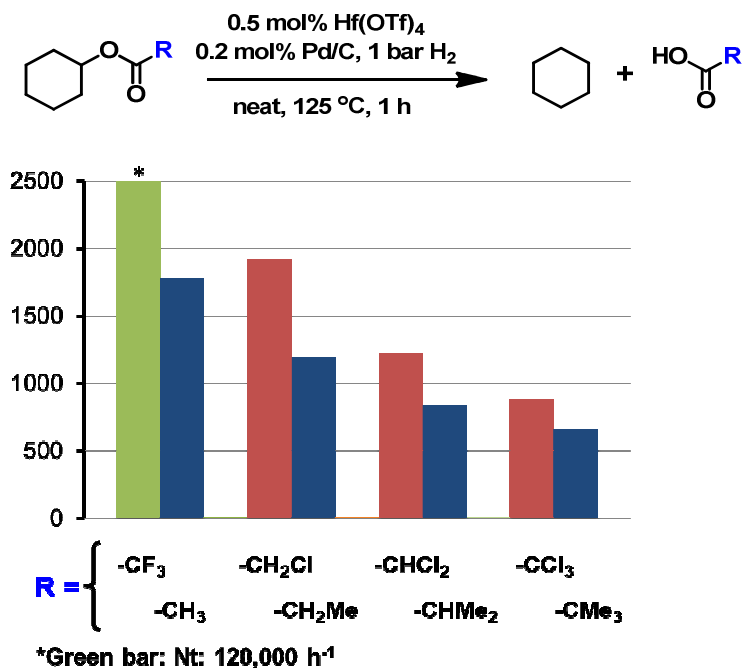


**Figure 4.** Influence of acyl substituent on ester hydrogenolysis activity

1776 h$^{-1}$ (Me) to 660 h$^{-1}$ ($^t$Bu). Note however that replacing an acyl H with a single electron-withdrawing chloro group increases the TOF to 1920 h$^{-1}$ (CH$_2$Cl), while including a second chloro group (CHCl$_2$) depresses the TOF to 1224 h$^{-1}$. Fully chlorinating the methyl group (CCl$_3$) further depresses the TOF to 880 h$^{-1}$. These results indicate that the most reactive acyl moieties are those with relatively unencumbered electron-withdrawing substituents. Furthermore, appending even more strongly electron-withdrawing substituents such as trifluoro (CF$_3$) substantially increases the TOF relative to R = CH$_3$. In sum, these results indicate that electron-withdrawing groups which stabilize the RCOO$^-$ negative charge most enhance the ester hydrogenolysis turnover frequency.

Next, alkoxy group effects were examined and the results are briefly summarized in Figure 5. The alkoxy group identity has a far greater influence on the rate of ester cleavage than does the acyl moiety. For example, at 1 bar H$_2$ and 125 °C, primary esters such as *n*-octyl acetate do not undergo RC(O)O-R' bond hydrogenolysis. Increasing the temperature to 200 °C affords the desired RC(O)O-R' cleavage products in moderate conversion after 3 hours (See Ref. 35 for a more detailed discussion and further substrate scope). Secondary esters are more rapidly cleaved than primary, and undergo cleavage at 125 °C. Tertiary esters are very reactive, with (±)-α-terpinyl acetate reaching 100% conversion in 30 min at 1 bar H$_2$ and 125 °C (See ref 35 for
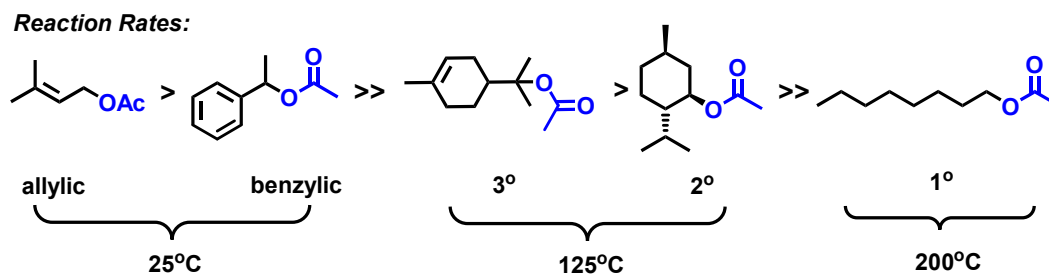


**Figure 5.** Influence of alkoxy group on catalytic ester hydrogenolysis activity

additional details). Benzylic and allylic esters are by far the most reactive substrates studied here. Substrates with accessible β-hydrogen atoms undergo rapid RC(O)O-R' bond cleavage, such as the secondary ester 1-phenylethyl acetate which achieves 98% conversion is 18 h at 25°C, and prenyl acetate is the most reactive substrate in the series, yielding 100% conversion in 10 min under 1 bar $H_2$ at 25°C[35]. In total, these results reveal a cleavage activity trend of 3° > 2° > 1° esters, with significant increases for benzylic and allylic esters, largely tracking the corresponding carbocation stability.[3]

*1.3 Kinetic and Mechanistic Studies of RC(O)O-R' Hydrogenolysis.* Quantitative kinetic studies of the representative RC(O)O-R' hydrogenolysis of the R = cyclohexyl derivative to acetic acid and cyclohexane were undertaken between 100 °C and 125 °C. Kinetic analysis was performed by periodically batch sampling < 0.1 mL aliquots of the neat reaction mixtures and analyzing by NMR spectroscopy in $CDCl_3$ using mesitylene (b.p. 165 °C) as an internal standard. The intermediate cyclohexene (b.p. 83 °C), and products acetic acid (b.p. 118 °C) and cyclohexane, (b.p. 81°C) were observed by NMR but not quantified due to their low boiling points.  The boiling point of cyclohexyl acetate is 173 °C.  Monitoring the hydrogenolysis of neat cyclohexyl acetate as a function of time in the presence of 0.50 mol % $Hf(OTf)_4$ and 0.20 mol% Pd/C (10 wt%) under 1 bar $H_2$ at 125 °C reveals linear substrate consumption (Figure 6A), suggesting zero-order dependence on substrate concentration . This indicates that under the applied conditions, the homogeneous metal triflate catalyst is operating under saturation kinetics. Monitoring the rate as a function of $H_2$ pressure reveals no significant dependence on $H_2$ pressure, indicating the reaction is zero order in $H_2$ concentration (Figure 6B) arguing that $H_2$ solubility affects are minimal. Finally, monitoring the reaction rate as a function of metal triflate concentration reveals a linear trend in

triflate concentration, indicating that the rate law is first-order in triflate catalyst. Therefore, the empirical rate law can be expressed as shown in eq. 1, arguing that the turnover- limiting step in RC(O)O-R' hydrogenolysis is C-O/C-H bond cleavage of the strongly bound RC(O)O···R'

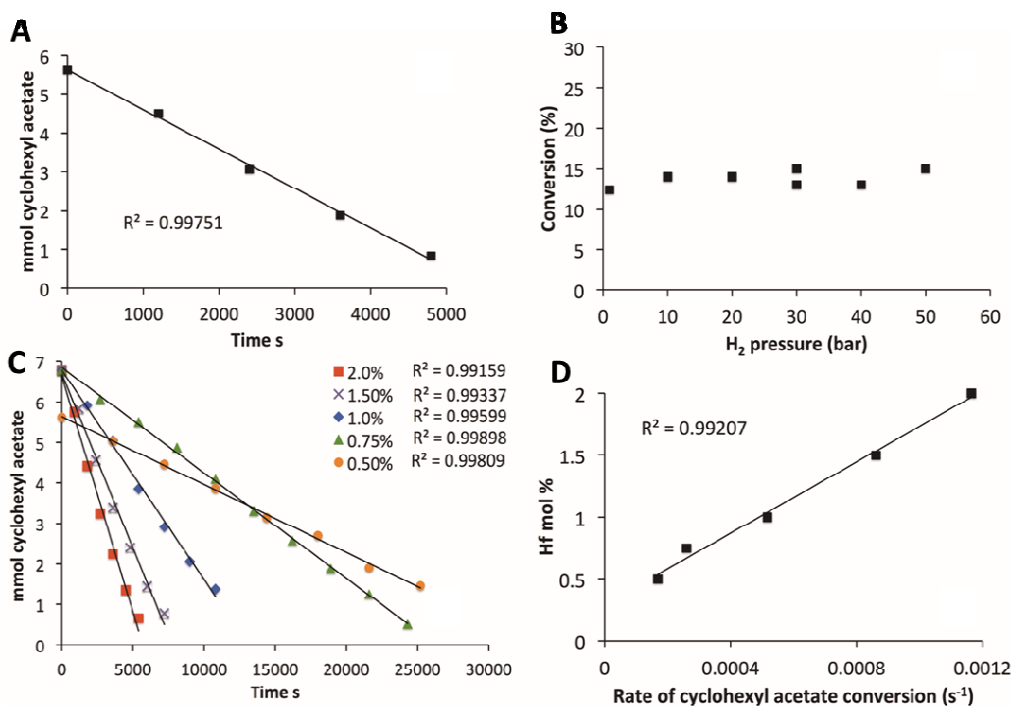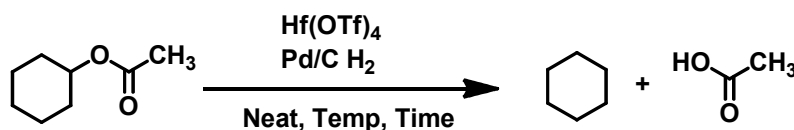$$\text{rate} = k[\text{substrate}]^0[H_2]^0[\text{metal triflate}]^1 \tag{1}$$



**Figure 6. A**. Plot of cyclohexyl acetate consumption versus time. Conditions: 120 °C, 0.50 mol % Hf(OTf)$_4$, 0.20 mol % Pd/C, 1 bar H$_2$. **B**. Conversion of cyclohexyl acetate as a function of H$_2$ pressure. Conditions: 1 hour, 100 °C, 0.50 mol % Hf(OTf)$_4$, 0.20 mol% Pd/C. **C**. Cyclohexyl acetate consumption versus time for different Hf(OTf)$_4$ catalyst loadings. Conditions: 100 °C, 1 bar H$_2$, catalyst ratio of 5:2 Hf:Pd for all. **D**. Plots of the rate of cyclohexyl acetate conversion as a function of Hf(OTf)$_4$ catalyst loading. Conditions: 100 °C, 1 bar H$_2$.

**Table 1.** Rate constants for the consumption of cyclohexyl acetate at different Hf(OTf)$_4$ mol% catalyst loadings and at different temperatures. Parentheses indicate uncertainty at the 95% confidence level.

| Temperature | Hf(OTf)$_4$ | Rate constant $k$ (x $10^{-3}$ s$^{-1}$) |
|---|---|---|
| 125 °C | 0.5% | 1.47 (6) |
| 120 °C | 0.5% | 1.02 (9) |
| 115 °C | 0.5% | 0.63 (8) |

| 110 °C | 0.5% | 0.38 (4) |
|--------|------|----------|
| 105 °C | 0.5% | 0.24 (2) |
| 100 °C | 0.5% | 0.168 (7) |
| 100 °C | 0.75% | 0.260 (7) |
| 100 °C | 1.0% | 0.49 (5) |
| 100 °C | 1.5% | 0.86 (8) |
| 100 °C | 2.0% | 1.2 (1) |

substrate. It will be seen below that this model is in agreement with DFT computation (*vide infra*), as is the derived rate law (see also Supporting Information).

Monitoring the model reaction of cyclohexyl acetate as a function of temperature by $^1$H NMR spectroscopy yields Eyring activation parameters (Figure 7), $\Delta H^\ddagger = 25(2)$ kcalmol$^{-1}$ and $\Delta S^\ddagger = -8(1)$ e.u. The small (in magnitude) negative $\Delta S^\ddagger$ in comparison to other known lanthanide-catalyzed hydroelementation/cyclization reactions, including, hydroamination, and hydrophosphination ($\Delta S^\ddagger \sim -19\text{-}27$ e.u.),[96] suggests a less ordered transition state, and is more
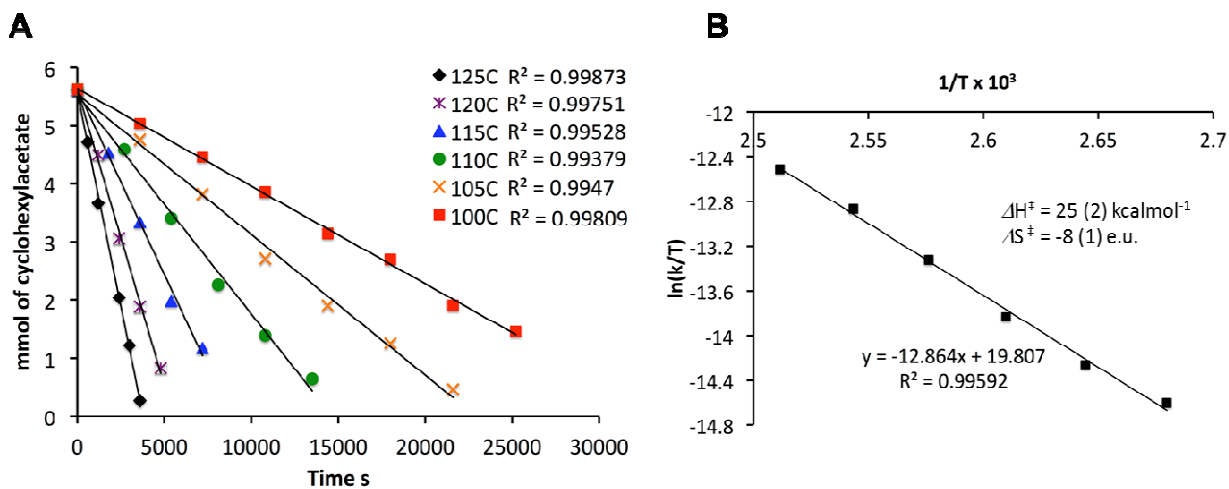


**Figure 7. A.** Plot of cyclohexyl acetate conversion versus temperature. Conditions: neat cyclohexyl acetate, 1 bar H$_2$, 0.5 mol % Hf(OTf)$_4$, 0.2 mol % Pd/C. **B.** Eyring analysis of cyclohexyl acetate conversion to yield activation parameters. Uncertainty estimated at the 95% confidence level.

reminiscent of triflate-mediated alkenol hydroalkoxlylations and ether hydrogenolyses ($\Delta S^\ddagger \sim -10\text{-}17$ e.u.).[97] The large energetic barrier indicated by the present $\Delta H^\ddagger$ is in accord with

substantial bond-breaking, uncompensated for by bond-making, as the transition state is approached. See more below in the DFT discussion.

*1.4 Kinetic and Equilibrium Isotope Effects*. The kinetic isotope effect (KIE) for ester hydrogenolysis was probed by comparing the cleavage rates of $d_4$-cyclohexyl acetate with that of the all-proteo isotopomer (Scheme 2). Performing the experiments at 1 bar $H_2$ and 125 °C with 0.50 mol% Hf(OTf)$_4$ reveals a substantial decrease in the rate of $d_4$-cyclohexyl acetate consumption versus that of the all-proteo isotopmer. Careful monitoring of the $^1$H NMR spectrum reveals formation of proteo acetic acid and that the cyclohexene intermediate is present in small quantities at high conversions. This suggests that the equilibrium constant (K$_1$) lies to the left under these reaction conditions and that the rate of ester-olefin equilibration is more rapid than subsequent hydrogenation. Therefore, we attribute the "apparent" KIE value obtained under these

**Scheme 2.** Kinetic and Equilibrium Isotope Effects ($k_A{}^+$ and $k_A{}^-$ represent the complexation and decomplexation of substrate to catalyst respectively; see Supporting Information for rate law derivation).
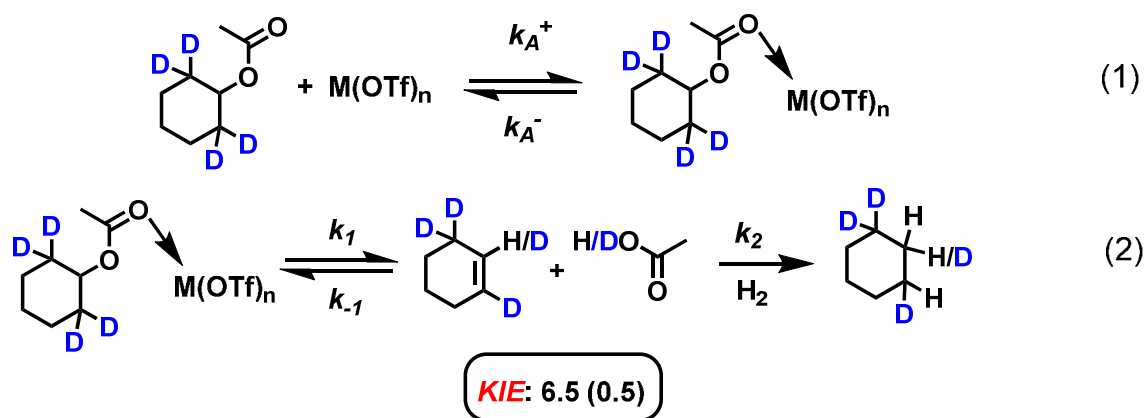


conditions (2.1(1)) to be complicated by an equilibrium isotope effect (EIE) resulting from the reversibility of the C-O cleavage step (k$_{-1}$). Therefore, to more accurately measure the KIE for the C-O cleavage step ($k_{1H}/k_{1D}$), the reaction was performed with a less active metal triflate,

catalyst, $Al(OTf)_3$, to slow the rapid equilibration in eq. 2 relative to cyclohexene hydrogenation, and with higher $H_2$ pressures (40 bar) to also ensure efficient cyclohexene capture. Under these conditions, the KIE = $6.5 \pm 0.5$, in good agreement with the DFT computation (see below).

*1.5.1 Triglyceride Hydrogenolysis.* Catalytic hydrogenolysis was next investigated with the model triglyceride tricaprylin (**5a**, Scheme 1, Figure 8) to assess those factors maximizing hydrogenolysis selectivity to diesters. Although 1,3-PDO dioctanoate (**7**), 1,2-PDO dioctanoate (**8**), and *n*-propyl octanoate (**9**) are observed in the final product mixture, the yields of all three are relatively modest using $Hf(OTf)_4$ as the Lewis acid because the triglyceride C3 backbone is converted predominantly to the ultimate hydrogenolysis product, propane. The yield of octanoic acid (**6**) reaches as high as 70 %, but is sacrificed via octanol formation at higher $H_2$ pressures (Table S2). Octanol in turn esterifies to form n-octyl octanoate (**10**) and water, which is utilized widely as a food additive,[98] in cosmetics,[99] and as a lubricant.[100] Interestingly, high temperatures (200 °C) but lower $H_2$ pressure (1 bar) afford cleaner conversion to propane and **6a**. At 200 °C and 1 bar $H_2$, the 49.7% conversion is achieved in 2 h (Table S2), while tripling the $Hf(OTf)_4$ loading further increases conversion to 86.2% (Table S2, Fig. 8C). Although the 2 h conversion is high, the combined condensed phase intermediates **7a-9a** only account for 12.0% of the total $C_3$ content, indicating that most of the $C_3$ is converted to gases. Analysis of the gaseous products reveals that propane comprises >96.0% of the carbonaceous products ($C_3H_8 \gg C_2H_6 > CO_2$, $CH_4$, $C_2H_4$, $C_3H_6$,), indicating minimal C-C cleavage (Fig. 8C). Trace $CO_2$ presumably arises from fatty acid decarboxylation.[101] Finally, for converting the fatty acid products to FAMEs, $Hf(OTf)_4$ is found here to be a highly efficient esterification catalyst,[102] affording complete conversion of **6a** with excess methanol to the corresponding methyl ester by stirring in the same reaction vessel at 25°C for 4 h.

1.5.2 *Tricaprylin hydrogenolysis product selectivity*. A systematic investigation of $C_3$ selectivity

to **7a**, **8a**, and **9a** was undertaken by screening catalysts of varying ionic radius and at various $H_2$

pressures at different levels of conversion (Figure 8B, Tables 2, 3, and S3), to understand those

factors which maximize **7a**, **8a**, and **9a** yields (Figure 8A). Optimal selectivity to 1,3-PDO

dioctanoate (**7a**), the most valuable C3 intermediate, is determined to be at 63-74% conversion at
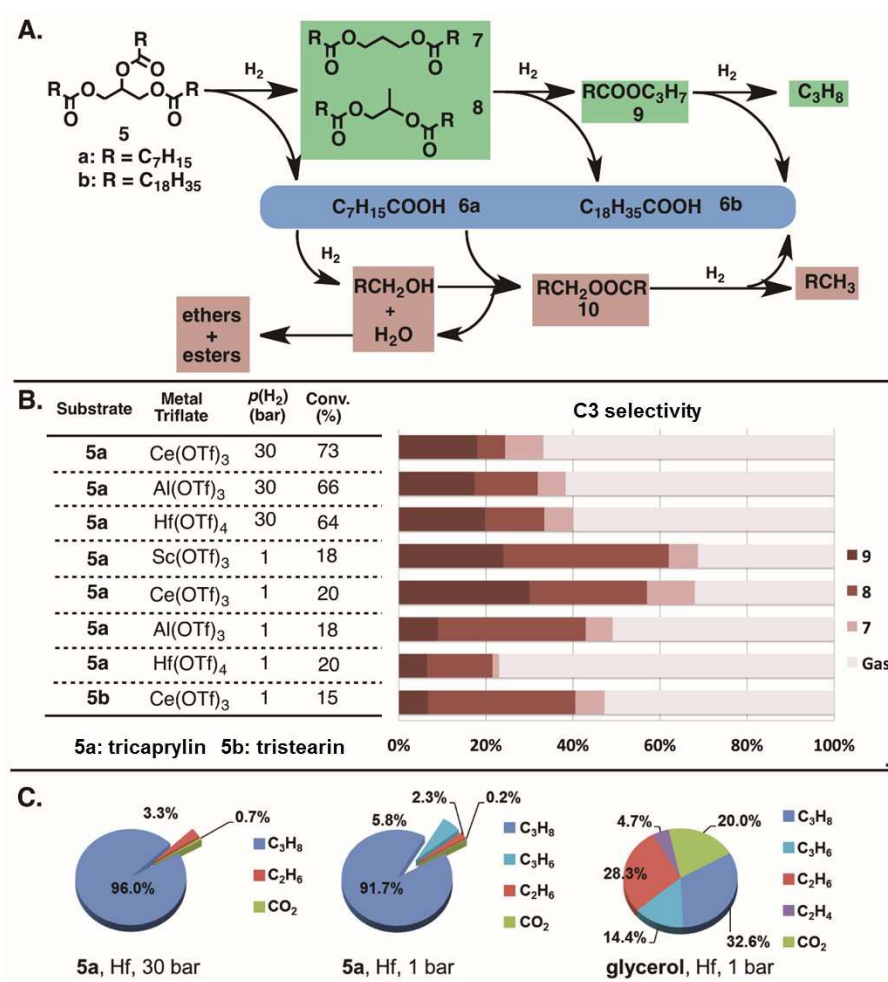


**Figure 8.** Tandem catalytic triglyceride hydrogenolysis data. **A.** Reaction network of tricaprylin (**5a**) hydrogenolysis mediated by the tandem $Hf(OTf)_4$ + Pd/C catalyst. **B.** Hydrogenolysis conditions and $C_3$ product selectivity. All reactions performed at the indicated $H_2$ pressure and 200 °C for 2 h. Catalyst loading for Line 1: 0.5 mol% $Hf(OTf)_4$, 0.2 mol% of 10% Pd/C; for the rest entries: 1.5 mol% metal triflate and 0.6 mol% of 10% Pd/C. **C.** Gaseous phase product distributions for **5a** hydrogenolysis at 30 and 1 bar $H_2$, and glycerol hydrogenolysis at 1 bar $H_2$.

30 bar $H_2$ and at 18-20 % conversion at 1 bar $H_2$ (Tables 2 and 3 and Figure S1). $C_3$ selectivity in these conversion ranges is shown in Figure 8B for a series of metal triflates. The selectivity to **7a** is highest at higher temperature (200 °C), with $Ce(OTf)_3$ Achieving the highest selectivity at both 30 bar (8.8%) and 1 bar (11%) $H_2$. Selectivity to **7a** increases with decreasing Lewis acid strength and metal triflate ionic radius (Ce ~ Sc > Al > Hf) at both 30 and 1 bar of $H_2$. Increasing $H_2$ pressure significantly increases the **9a** and **10a** yields (Tables 2 and S3), presumably reflecting the low reactivity of primary esters and increased propensity for **6a** hydrogenation at higher $H_2$ concentrations. Interestingly, high temperature (200 °C) but low $H_2$ pressure (1 bar) affords the highest selectivity to **7a** (Figures 8B, S1, and Table 3). Using $Ce(OTf)_3$, the $C_3$ selectivity to 1,3-PDO octanoate reaches a maximum of 11% as well as 27% for the 1,2-PDO octanoate product at 20% conversion (Figure 8B and Table 3 entry 9). Combined, the diester selectivity reaches as high as 48% (at 36% conversion) with $Ce(OTf)_3$ at 1 bar $H_2$ (Table 3 entry 10). With $Ce(OTf)_3$ identified as the most selective catalyst for **7a** at 1 bar $H_2$, the metal triflate to hydrogenation catalyst ratio was varied to determine the optimal ratio between catalysts (Figure S2 and Table 3 entries 12 and 13). Increasing or decreasing the amount of heterogeneous
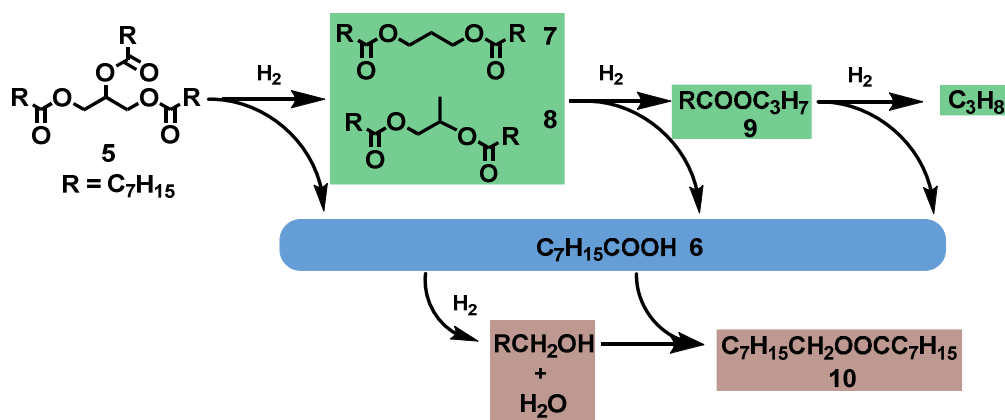


**Table 2**. Effect of Lewis acid catalyst on selectivity over a range of conversions at 200 °C and 30 bar $H_2$ for **5** (tricaprylin, R = $C_7H_{15}$, C3 selectivity in brackets).

| | $M(OTf)_n$ | Conv (%) | Liquid Phase Yield % (C3 selectivity) | | | | | "RCOO" Balance |
|---|---|---|---|---|---|---|---|---|
| | | | 6 | 7 | 8 | 9 | 10 | |

|  |  |  |  |  |  |  |  | (%) |
|---|---|---|---|---|---|---|---|---|
| 1[b] | Hf | 17 | 9 | - (0%) | 2.4(14%) | 1.5(8.8%) | 2.3 | 96.2 |
| 2[b] | Hf | 40 | 20.7 | 0.3(0.8%) | 8.1(20%) | 6.3(16%) | 6.2 | 96.4 |
| 3[b] | Hf | 64 | 40 | 4.3(6.7%) | 8.7(13.6%) | 12.7(20%) | 8.8 | 95 |
| 4[b] | Hf | 74 | 51.7 | 3.9(5.2%) | 4.8(6.5%) | 17.1(23%) | 12.2 | 100 |
| 5[b] | Hf | 96.7 | 69.8 | 4.5(4.7%) | 0.6(4%) | 21(21.6%) | 12.6 | 94 |
| 6[c] | Al | 25 | 12.2 | 1.8(7.2%) | 4.8(19.2%) | 2.2(8.8%) | 3.6 | 95.7 |
| 7[c] | Al | 66 | 41 | 4.2(6.4%) | 9.6(14.5%) | 11.5(17%) | 10.7 | 97.3 |
| 8[c] | Al | 86.8 | 58.5 | 6(6.9%) | 5.7(6.6%) | 20.8(24%) | 13.7 | 100 |
| 9[c] | Al | 94 | 52.5 | 6.3(6.7%) | 1.8(1.9%) | 22.9(24%) | 20.7 | 92.2 |
| 10[d] | Ce | 20 | 11.7 | 0.8(3.6%) | 3.9(17.7%) | 2.8(13%) | 4.9 | 98.7 |
| 11[d] | Ce | 73 | 48 | 4.3(5.6%) | 8.4(11.5%) | 8.7(12%) | 13 | 99.8 |
| 12[d] | Ce | 93.4 | 52 | 8.2(8.8%) | 6.0(6.4%) | 16.9(18%) | 23.1 | 96.9 |
| 13[e] | Ce | 95.8 | 55 | 1.6(1.7%) | 5.4(5.6%) | 17.4(18%) | 25.1 | 94.9 |
| 14[f] | Mg | 5 | 2.6 | 0.3(6%) | 0.9(18%) | 0.6(12%) | 0.5 | 99.2 |

[a] Conditions unless otherwise noted: 1.5 mol % $M(OTf)_3$, 0.6 mol% Pd/C and 1 mmol substrate in 2 mL cyclohexane at 200 °C in a 100 mL Parr reactor. [b] Reactions with $Hf(OTf)_4$ were run with 0.5 mol % $Hf(OTf)_4$ and 0.2 mol % Pd/C, for 30 min, 1.0 h, 1.5 h, 1.75 min, and 2.0 h to achieve conversions levels between 17% and 96.7%. [c] Reactions with $Al(OTf)_3$ were run for 30 minutes, 1.0 h, 1.75 h, and 2.0 h to achieve conversion levels between 25 and 94%. [d] Reactions with $Ce(OTf)_3$ run for 30 min, 2.0 h, and 4.0 h to achieve conversion levels between 20% and 93.4%. [e] Conditions: 2mL $ClCH_2CH_2Cl$ for 2.0 h. [f] 5.0 h.

**Table 3**. Effect of Lewis acid catalyst on selectivity over a range of conversions at 200 °C and 1 bar $H_2$ for **5** (tricaprylin, $R = C_7H_{15}$, C3 selectivity in brackets).

|  | $M(OTf)_n$ | Conv (%) | Liquid Phase Yield % (C3 selectivity) |  |  |  |  | "RCOO" Balance (%) |
|---|---|---|---|---|---|---|---|---|
|  |  |  | 6 | 7 | 8 | 9 | 10 |  |
| 1[b] | Hf | 20 | 12.6 | 0.3(1.5%) | 3(15%) | 1.3(6.5%) | 1.2 | 96.4 |
| 2[b] | Hf | 48.7 | 37.4 | 1.6(3.2%) | 1.2(2.5%) | 3.9(8%) | 1.2 | 93 |
| 3[b] | Hf | 86.2 | 48.9 | 4(4.6%) | 2.5(2.9%) | 5.5(6%) | 3.6 | 72 |
| 4[c] | Al | 18 | 4.8 | 1.1(6.2%) | 6(33.9%) | 1.6(9%) | 2.1 | 94.5 |
| 5[c] | Al | 27 | 11.5 | 1.5(5.5%) | 6.9(25.6%) | 4(14.4%) | 3.2 | 94.3 |
| 6[c] | Al | 41 | 37.1 | 3.9(9.5%) | 6.3(15.4%) | 4.5(11%) | 3 | 100 |
| 7[c] | Al | 53 | 27.6 | 3.1(5.8%) | 11(20.3%) | 7(13.6%) | 7.7 | 93.8 |
| 8[d] | Ce | 4 | 1.9 | -(0%) | 0.3(7.5%) | 0.3(7.5%) | 0.4 | 98.5 |
| 9[d] | Ce | 20 | 8.5 | 2.2(11%) | 5.4(27%) | 6.1(31%) | 2.4 | 97 |
| 10[d] | Ce | 36 | 17.2 | 3(8.3%) | 14.4(40%) | 6.7(19%) | 6.2 | 100 |
| 11[d] | Ce | 55 | 25 | 2.4(4.4%) | 16.2(30%) | 6.3(12%) | 9.9 | 95.6 |
| 12[de] | Ce | 15 | 6.5 | 1.3(8.7%) | 3.6(24%) | 0.6(4%) | 1.5 | 96 |
| 13[df] | Ce | 11 | 3.7 | 0.8(7.3%) | 2.1(19%) | 0.9(8.2%) | 1.2 | 96 |
| 14[g] | Sc | 15 | 6.3 | 0.5(3.3%) | 4.2(28%) | 2.1(4.7%) | 0.7 | 97 |
| 15[g] | Sc | 18 | 10 | 1.2(6.7%) | 6.9(38%) | 4.3(24%) | 4.8 | 100 |
| 16[g] | Sc | 28 | 11.3 | 1.8(6.4%) | 9.3(33%) | 3.7(13%) | 5.3 | 96.9 |

| 17[g] | Sc | 39 | 21 | 3(**7.7%**) | 15(**38%**) | 4.5(**11%**) | 6.1 | 100 |
| 18[g] | Sc | 53.5 | 34.3 | 3.4(**6.5%**) | 10.2(**19%**) | 10(**18.8%**) | 4.7 | 97.9 |
| 19[h] | Mg | - | - | - | - | - | - | - |

[a] Conditions unless otherwise noted: 1.5 mol % $M(OTf)_3$, 0.6 mol% Pd/C and 1 mmol substrate neat at 200 °C. [b] Reactions with $Hf(OTf)_4$ were run with 0.5 mol % $Hf(OTf)_4$ and 0.2 mol % Pd/C, for 30 min, 1.0 h, and 2.0 h to achieve conversions levels between 20% and 86.2%. [c] Reactions with $Al(OTf)_3$ were run at 30 min, 1.0 h, 2.0 h, and 4.0 h to achieve conversion levels between 18 and 53%. [d] Reactions with $Ce(OTf)_3$ were run at 30 min, 2.0 h, 4.0 h, and 6.0 h to achieve conversion levels between 4% and 55%. [e] Pd/C reduced to 0.3 mol%. [f] Pd/C loading doubled to 1.2 mol%. [g] Reactions with $Sc(OTf)_3$ were run at 2. h, 2.5 h, 4.0 h, 6.0 hours, and 8.0 h to achieve conversion levels between 15% and 53.5 %. [h] Reaction run for 17 h.

hydrogenation catalyst relative to $Ce(OTf)_3$ did not further enhance selectivity to **7a** (Table 3 entries 12 and 13, Figure S2). When the most selective low pressure catalytic protocol is next applied to tristearin (**5b**), a triglyceride animal fat derivative, slightly lower conversion and **7a** selectivity is observed over the same 2h time period, probably reflecting the lower solubility of $Ce(OTf)_3$ in neat tristearin (Fig. 8B and Table S3).

In contrast to the clean ester reactivities described above, control experiments with neat glycerol generate significant amounts of gaseous ethylene, ethane, and $CO_2$, in addition to heavy coking and a complex mixture in the condensed phase, indicating extensive C-C cleavage and deactivation of the Pd hydrogenation catalyst (Fig. 8C).

## 2. Discussion

*2.1 Mono-ester substrates.* A major goal of this contribution is to explore the scope and generality of metal triflate/supported Pd ester RC(O)O-R' bond cleavage, as well as to determine which factors most influence the activity and selectivity of this transformation. From the results in Figure 3, metal triflate catalytic activity increases with increased computed effective charge density ($p$) on the metal center, a result also observed for ether hydrogenolysis.[85, 86] Exploring different hydrogenation catalysts (Table S1) reveals that the Lewis basicity of the catalyst support is of paramount importance, since non-Lewis basic carbon and $SiO_2$ exhibit the highest

activity while more basic $Al_2O_3$ and $CeO_2$ suppress activity. This likely reflects competing Lewis acid-base interactions with the metal triflate, which in the case of $CeO_2$, renders the metal triflate completely inactive (Table S1). Alternatively, changing the Pd catalyst support may diminish the intrinsic hydrogenation activity,[93-95] however, kinetic results indicate that hydrogenation is typically not the turnover-limiting step, so this is probably not the case. Addition of Lewis basic solvents such as THF or MeOH have the same effect and result in triflate catalyst deactivation.

Varying the substituents on the carboxylate moiety effect large changes in catalytic turnover rates. Thus, increasing the steric bulk from $-CH_3$ to $-C(CH_3)_3$ in the acyl α-position significantly depresses the rate (Figure 4) implying that steric congestion impedes ester activation at the metal triflate center. Likewise, introducing electron-withdrawing groups on the acyl α-carbon position provides information on cleavage electronic requirements. Thus, a single -Cl atom results in a slight rate acceleration, consistent with electron-withdrawing substituents stabilizing the emerging carboxylate anion. Subsequently increasing the substitution to $-CHCl_2$ and $-CCl_3$ slightly decreases the reaction rate, presumably reflecting the interplay of electronic and steric effects. In contrast, for $-CF_3$ electronic effects clearly prevail and the reaction rate increases dramatically versus $-CH_3$.

Varying the alkoxy moiety (-OR') also has a large influence on the rate of ester RC(O)O-R' cleavage. Under standard reaction conditions (125 °C, 1 bar $H_2$) primary esters do not undergo hydrogenolysis with the present catalyst system. Instead, small amounts of ethers are produced, presumably via ester hydrolysis with trace water to afford the corresponding acid and alcohol, with the latter self-condensing to form ethers. However, significant primary ester RC(O)O-R' cleavage occurs when the temperature is raised to 200 °C, while secondary and tertiary esters

undergo hydrogenolysis at 125 °C/1 bar H$_2$, with tertiary being more reactive than secondary. Finally, R" = allylic and benzylic esters cleave very rapidly at room temperature.

Recently, Lohr et al., reported a preliminary mechanistic analysis of Hf(OTf)$_4$-mediated cycohexyl acetate hydrogenolysis using DFT computation.[34b,c,35]　In Figure 9, the computed enthalpic profiles (steps A to G) for the C-O bond cleavage of cyclohexyl acetate (A-CH$_3$ to G-CH$_3$) and cyclohexyltriflouroacetate　(A-CF$_3$ to G-CF$_3$) substrates are compared.　Regardless of the substrate, the steps associated with the deduced mechanistic pathway are similar: (A→B): exothermic binding of the substrate; (B→C→ D): C-O bond cleavage of the substrate via transition state C (TS1); (D→E→ F): formation of cyclohexene and carboxylic acid (coordinated
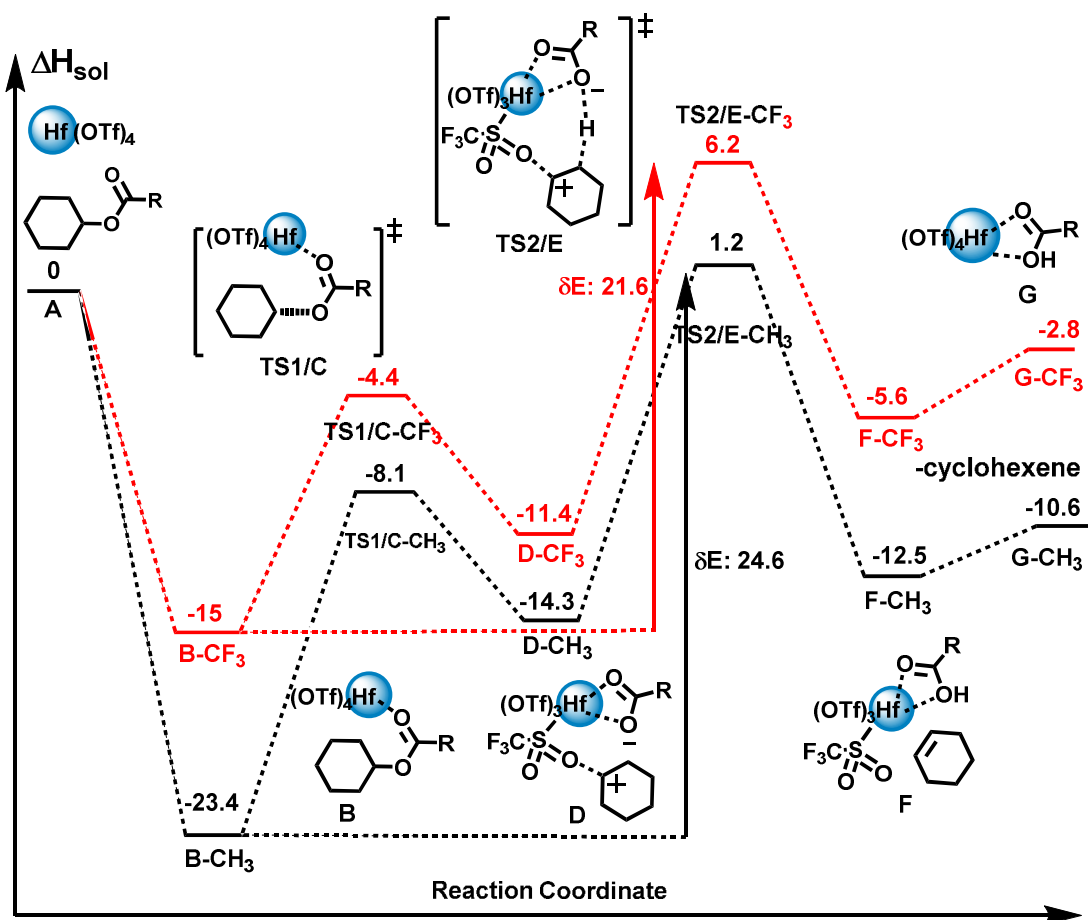


**Figure 9**. Comparison of the DFT-computed enthalpy profiles for RC(O)O-R' bond cleavage of cyclohexyl acetate (black) and cyclohexyl trifluoroacetate (red) catalyzed by Hf(OTf)$_4$.　A dielectric continuum model is used for the solvation.

to Hf); transition state E (TS2): proton transfer from the cationic cyclohexyl moiety to the carboxylate ion; (F→ G): cyclohexene dissociation carboxylic acid coordination to Hf(OTf)$_4$. The computed apparent activation enthalpy for cyclohexyl acetate using an *energy span* approach[103] is 24.6 kcal/mol; $\Delta H$(E-B) is in excellent agreement with the experimental value of 25(2) kcal/mol. Thus, based on the energy profile, the rate-limiting step traverses a triflate-stabilized carbocationic intermediate (transition state structure, TS2/E of Figure 9). Therefore, the rate of RC(O)O-R' bond cleavage correlates well with the stability of TS2/E produced by C-O cleavage, where a more substituted carbocation is more stable and lowers the energy of the transition state. By characterizing the RC(O)O-R' bond hydrogenolysis experimentally and computationally, the overall mechanism of this transformation as catalyzed by a tandem Lewis acid metal triflate/heterogeneous Pd catalyst can be proposed. Kinetic analysis shows that the reaction is first-order in [M(OTf)$_n$] catalyst, zero-order in [H$_2$], and zero-order in [substrate]. The first-order dependence on [M(OTf)$_n$] is consistent with the turnover-limiting step involving the RC(O)-OR cleavage, with the zero-order dependence on [H$_2$] consistent with hydrogenation following the turnover-limiting step. Zero-order behavior in [substrate] argues that substrate capture is rapid and essentially irreversible, and is consistent with the DFT-computed mechanism that involves proton transfer from the bound, triflate-stabilized cyclohexyl cation to the (TfO)$_4$Hf-coordinated carboxylate anion (Figure 9), consistent with the large experimental and computed primary kinetic isotope effect.

As seen from Figure 4, substituting the carboxylate CH$_3$ moiety for a more electron-withdrawing CF$_3$ group greatly accelerates the RC(O)O-R' cleavage rate, which is counterintuitive in that the CF$_3$COO$^-$ anion should be less basic than CH$_3$COO$^-$, and as such, might be expected to be less active for H$^+$ abstraction. Therefore the energetic pathway for the -

CF$_3$ derivative was computed to compare with that of the acetate, to determine the origin of the enhanced reactivity. The shape of the enthalpy and free energy (Figure 9 and Table S4 of the SI) profile for the cylochexyl trifluoroacetate is found to the similar to that of the cyclohexyl acetate. The first major -CF$_3$ effect is decreased stabilization of the bound catalyst/substrate complex (**B-CF$_3$**), presumably due to the reduced carboxylate basicity. Interestingly, the net result is a reduction of barrier to RC(O)O-R' cleavage (**C-CF$_3$**, TS1). For the same electronic reasons, the electron-withdrawing -CF$_3$ group destabilizes the carboxylate-Hf(OTf)$_4$-carbocation species (**D-CF$_3$**), which in turn lowers the overall barrier to H$^+$ transfer (**B-CF$_3$→E-CF$_3$**, TS2) versus the -CH$_3$ system. Thus, while H$^+$ transfer to the less basic coordinated CF$_3$COO$^-$ anion has a greater barrier (6.2 kcalmol$^{-1}$) than to CH$_3$COO$^-$ (1.2 kcalmol$^{-1}$), this is more than compensated for by destabilization of the substrate-bound catalyst species (**B-CF$_3$** and **D-CF$_3$**), resulting in a net lowering of the apparent enthalpic barrier to 21.2 kcalmol$^{-1}$ for cyclohexyl trifluoroacetate from 24.6 kcalmol$^{-1}$ in cyclohexyl acetate, in agreement with the experimental kinetic data.

*2.2 Triglycerides.* Mechanistically, ester hydrogenolysis here follows trends reminiscent of simpler tandem metal triflate Lewis acid/Pd-catalyzed ether and monoester hydrogenolysis. First, weaker Lewis acids such as Al(OTf)$_3$, Ce(OTf)$_3$, or Sc(OTF)$_3$, or Lewis basic additives/solvents such as *N,N*-dimethylacetamide, THF, and H$_2$O, substantially depress cleavage rates (Tables S1 and S3), highlighting the crucial role triflate Lewis acidity plays in the catalytic process. Second, significant yields of propylene are detected in the gas phase over the reaction mixture at 1 bar of H$_2$, implicating carboxylate elimination to produce alkene (Fig. 8C). Lastly, the present reaction does not generate carbon-containing gases without the presence of Pd/C, indicating that a tandem combination of catalysts is necessary (Table S3). Exploration of the electronic and steric factors governing ester RC(O)O-R' bond cleavage by metal triflates provides information relevant to the

selectivity of triglyceride conversion. A priori, in accordance with model substrates, secondary or internal ester RC(O)O-R' bond cleavage should be more rapid than primary, or terminal, ester cleavage. However, triglyceride primary/terminal cleavage predominates over secondary/internal cleavage at all temperatures examined. From model substrates, it is evident that RC(O)O-R' cleavage rates are sensitive to steric congestion (Figure 5), and is reasonable to propose that cleavage rates at the secondary/internal ester position are compromised by steric congestion versus that at a primary terminal position. Moving to less acidic metal triflates (Figure 8B and Tables 2 and 3) does increase the selectivity to secondary internal cleavage, doubling from 5.4% for $Hf(OTf)_4$ to 9.5% for $Al(OTf)_3$ and 11% for $Ce(OTf)_3$. The maximum combined selectivity to diesters (1,2 + 1,3) is found to be 48% using $Ce(OTf)_3$ at 1 bar $H_2$.

The experiments on model allylic monoesters are also informative (Figure 5). Allylic monoesters are by far the most reactive, and undergo rapid RC(O)-OR' bond hydrogenolysis at 25°C. Thus, triglyceride allylic ester intermediates are also more likely to undergo rapid second RC(O)-OR' bond cleavage before hydrogenolysis (Scheme 3). Increasing the $H_2$ pressure to intercept the allylic intermediates at the 1,3 and 1,2-dioctanoate stage does not increase the selectivity to those products (Table 2). In accord with this picture, suppressing the rate of RC(O)O-R' cleavage versus hydrogenation using less active triflates (Al, Ce, Sc) doubles the selectivity to 1,3-dioctonoate, however, this may also reflect the steric factors noted above. It is probable that both sterics and allylic intermediates limit 1,3-dioctanoate selectivity here.

**Conclusions**

Using the tandem catalytic system described, the formation of undesired waste glycerol is blocked by "detouring" the $C_3$ backbone to more valuable products, a pressing issue in

32

**Scheme 3**. Possible reactive allylic intermediates in triglyceride hydrogenolysis
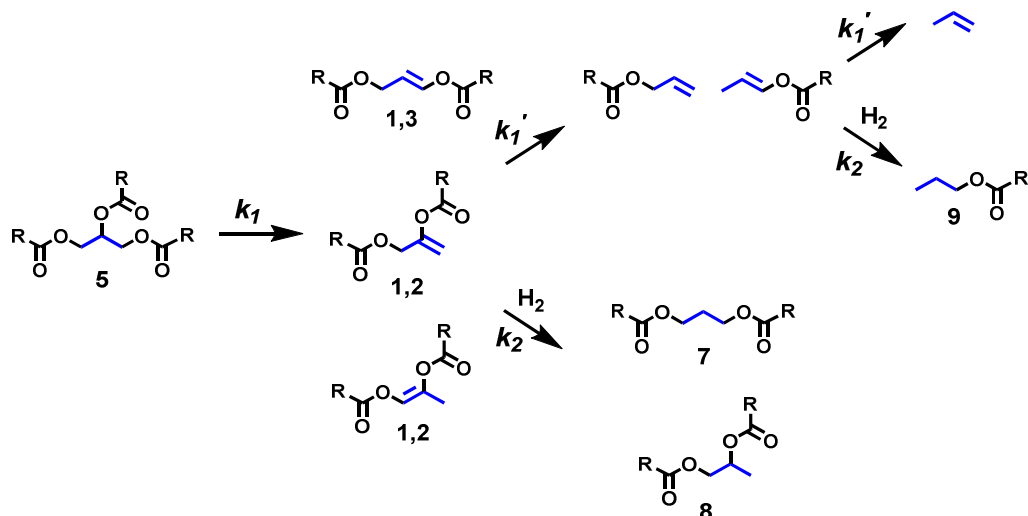


traditional biodiesel fuel production. Notably, this catalytic strategy yields the dioctanoates in up to 48 % selectivity (at 36% conversion) using $Ce(OTf)_3$ and a supported Pd hydrogenation catalyst. Alternatively, using $Hf(OTf)_4$ results in rapid conversions within 2 h to > 82 % gaseous $C_3$ products The present strategy represents a first step toward producing more valuable $C_3$ intermediates (1,2-PDO, 1,3-PDO, 1-propanol, propane) over low-value glycerol during biodiesel fuel production from triglycerides.

†**Electronic Supplementary Information (ESI) available: See DOI: 10.1039/x0xx00000x.**

## References

1. E. Barbayianni and G. Kokotos, *Chemcatchem*, 2012, **4**, 592.
2. D. S. Merel, D. Minh Loan Tran, S. Gaillard, P. Dupau and J.-L. Renaud, *Coord. Chem. Rev.*, 2015, **288**, 50.
3. M. Smith, *March's advanced organic chemistry : reactions, mechanisms, and structure*, Wiley, Hoboken, New Jersey, 7th Edition / edn., 2013.
4. K. A. Manbeck, S. Kundu, A. P. Walsh, W. W. Brennessel and W. D. Jones, *Organometallics*, 2012, **31**, 5018.
5. A. Srifa, K. Faungnawakij, V. Itthibenchapong, N. Viriya-Empikul, T. Charinpanitkul and S. Assabumrungrat, *Bioresour. Technol.*, 2014, **158**, 81.
6. S. Pinzi, D. Leiva, I. López-García, M. D. Redel-Macías and M. P. Dorado, *Biofuels, Bioproducts and Biorefining*, 2014, **8**, 126.
7. C. Wu, Z. Wang, L. Wang, J. Huang and P. T. Williams, *Waste and Biomass Valorization*, 2014, **5**, 175.
8. S. A. W. Hollak, M. A. Ariens, K. P. de Jong and D. S. van Es, *Chemsuschem*, 2014, **7**, 1057.
9. E. M. Krall, T. W. Klein, R. J. Andersen, A. J. Nett, R. W. Glasgow, D. S. Reader, B. C. Dauphinais, S. P. Mc Ilrath, A. A. Fischer, M. J. Carney, D. J. Hudson and N. J. Robertson, *Chem. Commun.*, 2014, **50**, 4884.
10. X. Cai, M. Sakamoto, M. Yamaji, M. Fujitsuka and T. Majima, *Chemistry-a European Journal*, 2007, **13**, 3143.
11. R. August, C. Davis and R. Taylor, *Journal of the Chemical Society, Perkin Transactions 2*, 1986, DOI: 10.1039/p29860001265, 1265.
12. Y. V. Subba Rao, P. Vijayanand, S. J. Kulkarni, M. Subrahmanyam and A. V. Rama Rao, *Synth. Commun.*, 1995, **25**, 849.
13. P. Gogoi, D. Konwar, S. Das Sharma and P. K. Gogoi, *Synth. Commun.*, 2006, **36**, 1259.
14. T. Yamamoto, J. Ishizu, T. Kohara, S. Komiya and A. Yamamoto, *J. Am. Chem. Soc.*, 1980, **102**, 3758.
15. X. Hong, Y. Liang and K. N. Houk, *J. Am. Chem. Soc.*, 2014, **136**, 2017.
16. T. Yamamoto, S. Miyashita, Y. Naito, S. Komiya, T. Ito and A. Yamamoto, *Organometallics*, 1982, **1**, 808.
17. G. A. T. Hoang, V. J. Reddy, H. H. K. Nguyen and C. J. Douglas, *Angewandte Chemie-International Edition*, 2011, **50**, 1882.

18.     Y. J. Zhu, D. A. Smith, D. E. Herbert, S. Gatard and O. V. Ozerov, *Chem. Commun.*, 2012, **48**, 218.
19.     K. Nagayama, I. Shimizu and A. Yamamoto, *Bull. Chem. Soc. Jpn.*, 1999, **72**, 799.
20.     Y. S. Bao, C. Y. Chen and Z. Z. Huang, *J. Org. Chem.*, 2012, **77**, 8344.
21.     Y. S. Bao, B. Zhaorigetu, B. Agula, M. H. Baiyin and M. L. Jia, *J. Org. Chem.*, 2014, **79**, 803.
22.     B.-J. Li, L. Xu, Z.-H. Wu, B.-T. Guan, C.-L. Sun, B.-Q. Wang and Z.-J. Shi, *J. Am. Chem. Soc.*, 2009, **131**, 14656.
23.     M. Solecki, A. Scodel and B. Epstein, *Advanced Biofuel Market Report 2013 - Capacity through 2016*, 2013.
24.     R. S. Srivastava, *Appl. Organomet. Chem.*, 1993, **7**, 607.
25.     J. G. Planas, T. Marumo, Y. Ichikawa, M. Hirano and S. Komiya, *Journal of the Chemical Society-Dalton Transactions*, 2000, DOI: 10.1039/b002428g, 2613.
26.     G. Ferrando, J. N. Coalter, H. Gerard, D. J. Huang, O. Eisenstein and K. G. Caulton, *New J. Chem.*, 2003, **27**, 1451.
27.     X. Tan, Y. Wang, Y. Liu, F. Wang, L. Shi, K.-H. Lee, Z. Lin, H. Lv and X. Zhang, *Org. Lett.*, 2015, **17**, 454.
28.     X. Tan, Q. Wang, Y. Liu, F. Wang, H. Lv and X. Zhang, *Chemical communications (Cambridge, England)*, 2015, **51**, 12193.
29.     D. Spasyuk, C. Vicent and D. G. Gusev, *J. Am. Chem. Soc.*, 2015, **137**, 3743.
30.     M. Hirano, S. Kawazu and N. Komine, *Organometallics*, 2014, **33**, 1921.
31.     T. Ito, T. Matsubara and Y. Yamashita, *Journal of the Chemical Society-Dalton Transactions*, 1990, DOI: 10.1039/dt9900002407, 2407.
32.     B. T. Guan, Y. Wang, B. J. Li, D. G. Yu and Z. J. Shi, *J. Am. Chem. Soc.*, 2008, **130**, 14468.
33.     K. W. Quasdorf, X. Tian and N. K. Garg, *J. Am. Chem. Soc.*, 2008, **130**, 14422.
34.     L. Xu, B.-J. Li, Z.-H. Wu, X.-Y. Lu, B.-T. Guan, B.-Q. Wang, K.-Q. Zhao and Z.-J. Shi, *Org. Lett.*, 2010, **12**, 884.
35.     H. K, S.-F. Yu Dg Fau - Zheng, Z.-H. Zheng Sf Fau - Wu, Z.-J. Wu Zh Fau - Shi and S. ZJ, *Chemistry*, 2011, **17**, 786.
36.     S. Kundu, J. Choi, D. Y. Wang, Y. Choliy, T. J. Emge, K. Krogh-Jespersen and A. S. Goldman, *J. Am. Chem. Soc.*, 2013, **135**, 5127.
37.     Y. Ogiwara, M. Tamura, T. Kochi, Y. Matsuura, N. Chatani and F. Kakiuchi, *Organometallics*, 2014, **33**, 402.
38.     H. Juteau and Y. Gareau, *Synth. Commun.*, 1998, **28**, 3795.
39.     A. T. Madsen, E. Ahmed, C. H. Christensen, R. Fehrmann and A. Riisager, *Fuel*, 2011, **90**, 3433.
40.     J. Han, H. Sun, Y. Ding, H. Lou and X. Zheng, *Green Chemistry*, 2010, **12**, 463.
41.     L. Boda, O. Gyorgy, H. Solt, L. Ferenc, J. Valyon and A. Thernesz, *Applied Catalysis a-General*, 2010, **374**, 158.
42.     W. J. Song, C. Zhao and J. A. Lercher, *Chemistry-a European Journal*, 2013, **19**, 9833.
43.     E. Santillan-Jimenez, T. Morgan, J. Lacny, S. Mohapatra and M. Crocker, *Fuel*, 2013, **103**, 1010.
44.     Q. Y. Liu, H. L. Zuo, T. J. Wang, L. L. Ma and Q. Zhang, *Applied Catalysis a-General*, 2013, **468**, 68.
45.     K. Kandel, C. Frederickson, E. A. Smith, Y. J. Lee and Slowing, II, *ACS Catalysis*, 2013, **3**, 2750.
46.     B. X. Peng, X. G. Yuan, C. Zhao and J. A. Lercher, *J. Am. Chem. Soc.*, 2012, **134**, 9400.
47.     B. X. Peng, Y. Yao, C. Zhao and J. A. Lercher, *Angewandte Chemie-International Edition*, 2012, **51**, 2072.
48.     Y. Y. Liu, R. Sotelo-Boyas, K. Murata, T. Minowa and K. Sakanishi, *Energy & Fuels*, 2011, **25**, 4675.
49.     S. K. Kim, J. Y. Han, H. S. Lee, T. Yum, Y. Kim and J. Kim, *Applied Energy*, 2014, **116**, 199.
50.     C. Zhao, T. Bruck and J. A. Lercher, *Green Chemistry*, 2013, **15**, 1720.
51.     R. W. Gosselink, S. A. W. Hollak, S. W. Chang, J. van Haveren, K. P. de Jong, J. H. Bitter and D. S. van Es, *Chemsuschem*, 2013, **6**, 1576.

52.    T. V. Choudhary and C. B. Phillips, *Applied Catalysis a-General*, 2011, **397**, 1.
53.    T. Morgan, D. Grubb, E. Santillan-Jimenez and M. Crocker, *Top. Catal.*, 2010, **53**, 820.
54.    B. Smith, H. C. Greenwell and A. Whiting, *Energy & Environmental Science*, 2009, **2**, 262.
55.    S. Lestari, P. Maki-Arvela, J. Beltramini, G. Q. M. Lu and D. Y. Murzin, *Chemsuschem*, 2009, **2**, 1109.
56.    V. B. Borugadda and V. V. Goud, *Renewable and Sustainable Energy Reviews*, 2012, **16**, 4763.
57.    E. U. Kiran, A. P. Trzcinski, W. J. Ng and Y. Liu, *Fuel*, 2014, **134**, 389.
58.    E. F. Aransiola, T. V. Ojumu, O. O. Oyekola, T. F. Madzimbamuto and D. I. O. Ikhu-Omoregbe, *Biomass Bioenergy*, 2014, **61**, 276.
59.    A. Abbaszaadeh, B. Ghobadian, M. R. Omidkhah and G. Najafi, *Energy Convers. Manage.*, 2012, **63**, 138.
60.    E. M. Shahid and Y. Jamal, *Renewable and Sustainable Energy Reviews*, 2011, **15**, 4732.
61.    L. C. Meher, D. Vidya Sagar and S. N. Naik, *Renewable and Sustainable Energy Reviews*, 2006, **10**, 248.
62.    M. Ayoub and A. Z. Abdullah, *Renewable and Sustainable Energy Reviews*, 2012, **16**, 2671.
63.    C.-H. Zhou, J. N. Beltramini, Y.-X. Fan and G. Q. Lu, *Chem. Soc. Rev.*, 2008, **37**, 527.
64.    Y. Nakagawa, M. Tamura and K. Tomishige, *Journal of Materials Chemistry A*, 2014, **2**, 6688.
65.    M. Besson, P. Gallezot and C. Pinel, *Chem. Rev.*, 2014, **114**, 1827.
66.    J. C. Beltrán-Prieto, K. Kolomazník and J. Pecha, *Aust. J. Chem.*, 2013, **66**, 511.
67.    M. Simões, S. Baranton and C. Coutanceau, *ChemSusChem*, 2012, **5**, 2106.
68.    J. v. Haveren, E. L. Scott and J. Sanders, *Biofuels, Bioproducts and Biorefining*, 2008, **2**, 41.
69.    M. Pagliaro, R. Ciriminna, H. Kimura, M. Rossi and C. Della Pina, *Angew. Chem. Int. Ed.*, 2007, **46**, 4434.
70.    Z. Y. Zakaria, N. A. S. Amin and J. Linnekoski, *Biomass Bioenergy*, 2013, **55**, 370.
71.    H. W. Tan, A. R. Abdul Aziz and M. K. Aroua, *Renewable and Sustainable Energy Reviews*, 2013, **27**, 118.
72.    C. A. G. Quispe, C. J. R. Coronado and J. A. Carvalho Jr, *Renewable and Sustainable Energy Reviews*, 2013, **27**, 475.
73.    F. Liu, K. De Oliveira Vigier, M. Pera-Titus, Y. Pouilloux, J.-M. Clacens, F. Decampo and F. Jerome, *Green Chemistry*, 2013, **15**, 901.
74.    J. Oh, S. Dash and H. Lee, *Green Chemistry*, 2011, **13**, 2004.
75.    L.-Z. Qin, M.-J. Song and C.-L. Chen, *Green Chemistry*, 2010, **12**, 1466.
76.    E. Arceo, P. Marsden, R. G. Bergman and J. A. Ellman, *Chem. Commun.*, 2009, DOI: 10.1039/b907746d, 3357.
77.    T. Kurosaka, H. Maruyama, I. Naribayashi and Y. Sasaki, *Catal. Commun.*, 2008, **9**, 1360.
78.    M. R. Nimlos, S. J. Blanksby, X. Qian, M. E. Himmel and D. K. Johnson, *The Journal of Physical Chemistry A*, 2006, **110**, 6145.
79.    K. Wang, M. C. Hawley and S. J. DeAthos, *Industrial & Engineering Chemistry Research*, 2003, **42**, 2913.
80.    A. Martin, U. Armbruster, I. Gandarias and P. L. Arias, *Eur. J. Lipid Sci. Technol.*, 2013, **115**, 9.
81.    B. Katryniok, S. Paul and F. Dumeignil, *ACS Catalysis*, 2013, **3**, 1819.
82.    N. H. Tran and G. S. K. Kannangara, *Chem. Soc. Rev.*, 2013, **42**, 9454.
83.    Y. Nakagawa and K. Tomishige, *Catalysis Science & Technology*, 2011, **1**, 179.
84.    A. C. Atesin, N. A. Ray, P. C. Stair and T. J. Marks, *J. Am. Chem. Soc.*, 2012, **134**, 14682.
85.    R. S. Assary, A. C. Atesin, Z. Li, L. A. Curtiss and T. J. Marks, *ACS Catal.*, 2013, **3**, 1908.
86.    Z. Li, R. S. Assary, A. C. Atesin, L. A. Curtiss and T. J. Marks, *J. Am. Chem. Soc.*, 2014, **136**, 104.
87.    T. L. Lohr, Z. Li, R. S. Assary, L. A. Curtiss and T. J. Marks, *Acs Catalysis*, 2015, **5**, 3675.
88.    E. Gaigneaux*, M. Devillers, S. Hermans, P. A. Jacobs, J. Martens and P. Ruiz, *Scientific Bases for the Preparation of Heterogeneous Catalysts: Proceedings of the 10th International Symposium, Louvain-la-Neuve, Belgium, July 11-15, 2010*, Elsevier Science, 2010.

89.     F. J. Waller, A. G. M. Barrett, D. C. Braddock and D. Ramprasad, *Tetrahedron Lett.*, 1998, **39**, 1641.

90.     M. Hatano, Y. Furuya, T. Shimmura, K. Moriyama, S. Kamiya, T. Maki and K. Ishihara, *Org. Lett.*, 2010, **13**, 426.

91.     M. J. T. Frisch, G. W.; Schlegel, H. B.; Scuseria, G. E.; Robb, M. A.; Cheeseman, J. R.; Montgomery, J. A.; Vreven, T.; Kudin, K. N.; Burant, J. C.; Millam, J. M.; Iyengar, S. S.; Tomasi, J.; Barone, V.; Mennucci, B.; Cossi, M.; Scalmani, G.; Rega, N.; Petersson, G. A.; Nakatsuji, H.; Hada, M.; Ehara, M.; Toyota, K.; Fukuda, R.; Hasegawa, J.; Ishida, M.; Nakajima, T.; Honda, Y.; Kitao, O.; Nakai, H.; Klene, M.; Li, X.; Knox, J. E.; Hratchian, H. P.; Cross, J. B.; Bakken, V.; Adamo, C.; Jaramillo, J.; Gomperts, R.; Stratmann, R. E.; Yazyev, O.; Austin, A. J.; Cammi, R.; Pomelli, C.; Ochterski, J. W.; Ayala, P. Y.; Morokuma, K.; Voth, G. A.; Salvador, P.; Dannenberg, J. J.; Zakrzewski, V. G.; Dapprich, S.; Daniels, A. D.; Strain, M. C.; Farkas, O.; Malick, D. K.; Rabuck, A. D.; Raghavachari, K.; Foresman, J. B.; Ortiz, J. V.; Cui, Q.; Baboul, A. G.; Clifford, S.; Cioslowski, J.; Stefanov, B. B.; Liu, G.; Liashenko, A.; Piskorz, P.; Komaromi, I.; Martin, R. L.; Fox, D. J.; Keith, T.; Laham, A.; Peng, C. Y.; Nanayakkara, A.; Challacombe, M.; Gill, P. M. W.; Johnson, B.; Chen, W.; Wong, M. W.; Gonzalez, C.; Pople, J. A. , 2009.

92.     L. Cervený, *Catalytic Hydrogenation*, Elsevier Science, 1986.

93.     C. Park and M. A. Keane, *J. Colloid Interface Sci.*, 2003, **266**, 183.

94.     M. Bauer, R. Schoch, L. Shao, B. Zhang, A. Knop-Gericke, M. Willinger, R. Schlögl and D. Teschner, *The Journal of Physical Chemistry C*, 2012, **116**, 22375.

95.     P. Rylander, *Catalytic Hydrogenation over Platinum Metals*, Elsevier Science, 2012.

96.     S. Y. Seo, X. H. Yu and T. J. Marks, *J. Am. Chem. Soc.*, 2009, **131**, 263.

97.     A. Dzudza and T. J. Marks, *Chemistry-a European Journal*, 2010, **16**, 3403.

98.     G. A. Burdock, *Encyclopedia of Food and Color Additives*, CRC-Press, 1997.

99.     A. O. Barel, M. Paye and H. I. Maibach, *Handbook of Cosmetic Science and Technology, Third Edition*, CRC Press, 2009.

100.    L. Urteaga, N. Sánchez, M. Martinez and J. Aracil, *Chemical Engineering & Technology*, 1994, **17**, 210.

101.    W. F. Maier, W. Roth, I. Thies and P. V. R. Schleyer, *Chem. Ber.*, 1982, **115**, 808.

102.    A. G. M. Barrett and D. Christopher Braddock, *Chem. Commun.*, 1997, DOI: 10.1039/A606484A, 351.

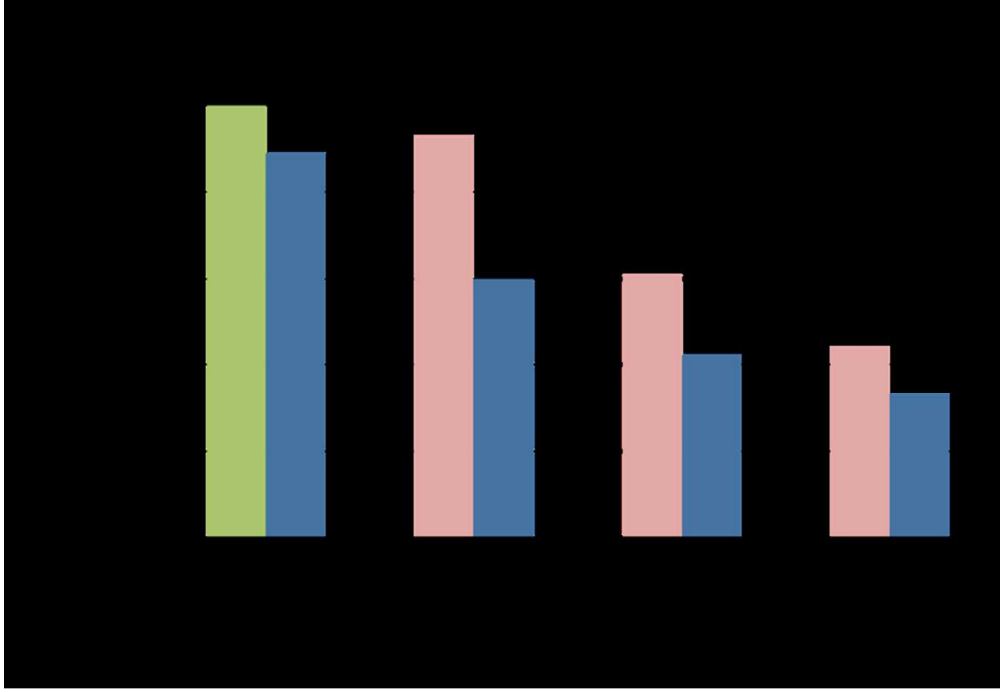103.    S. Kozuch and J. M. L. Martin, *Acs Catalysis*, 2012, **2**, 2787.

**TOC GRAPHIC**

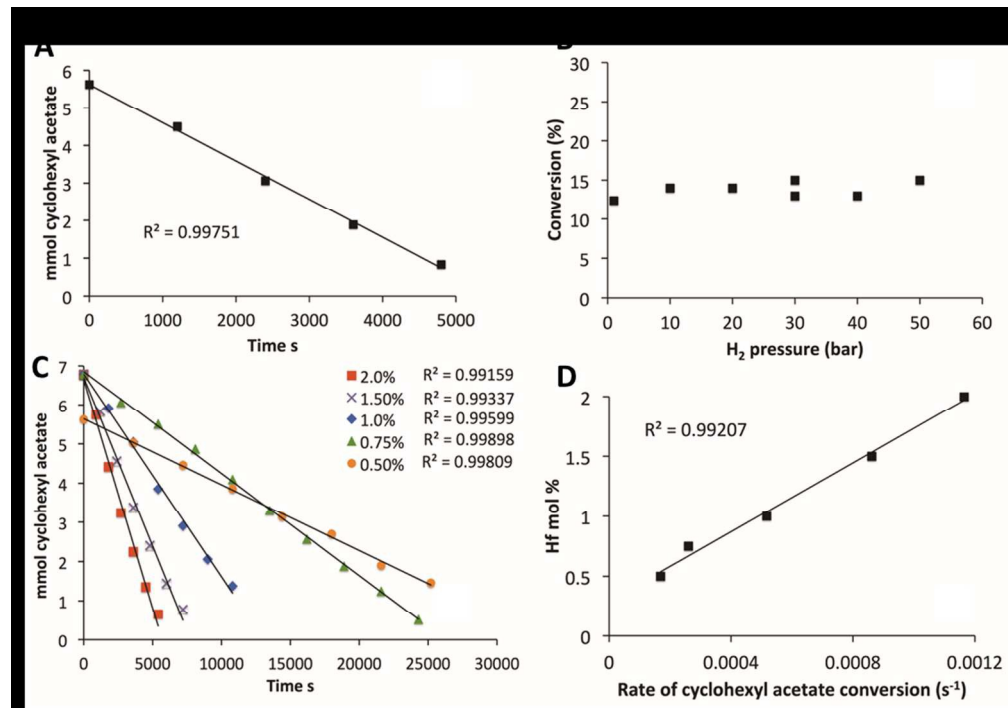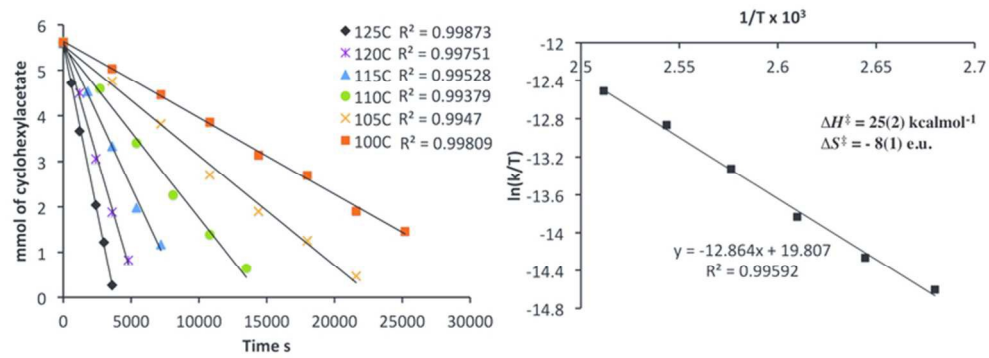*Understanding Ester Cleavage for Triglyceride Hydrogenolysis*
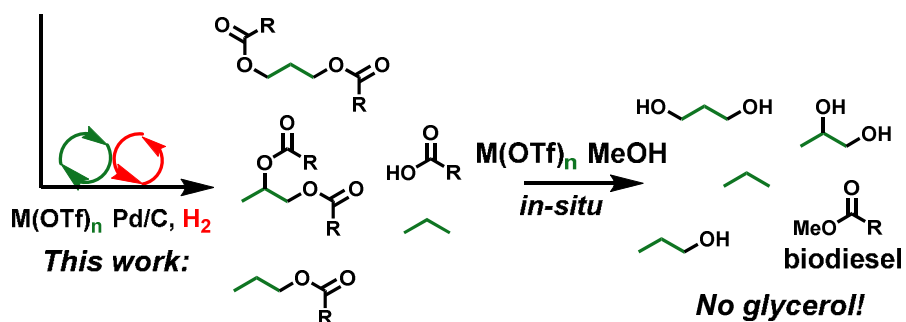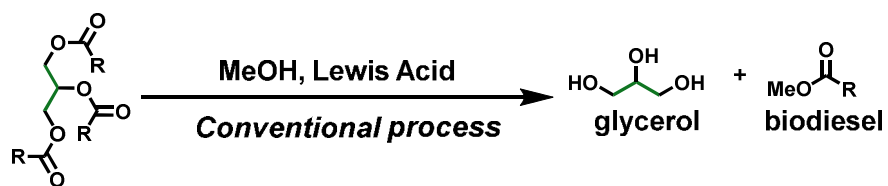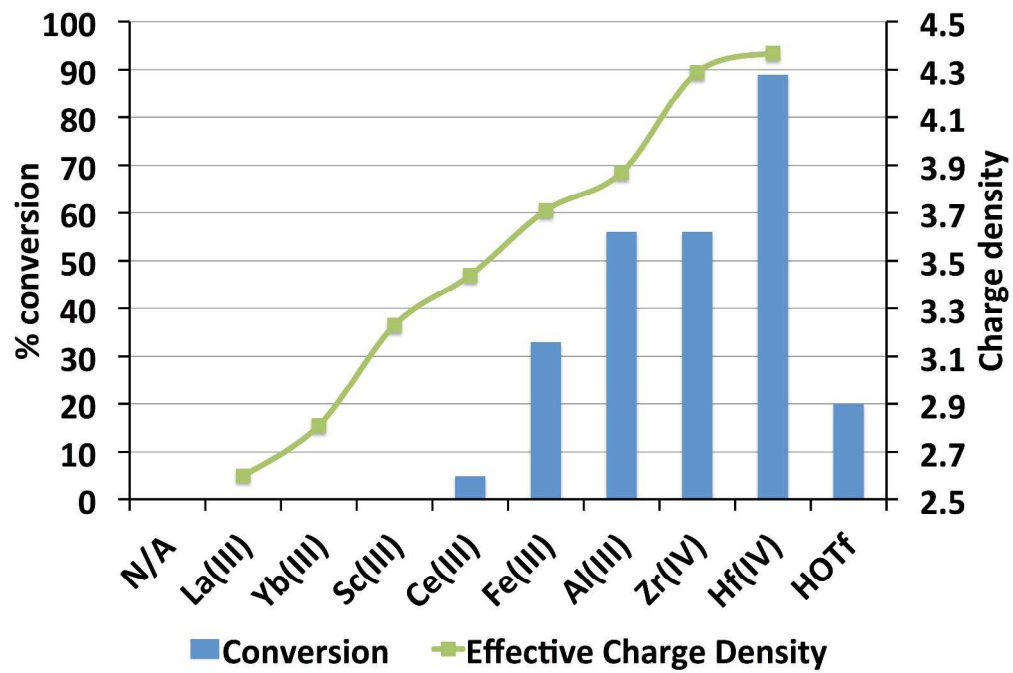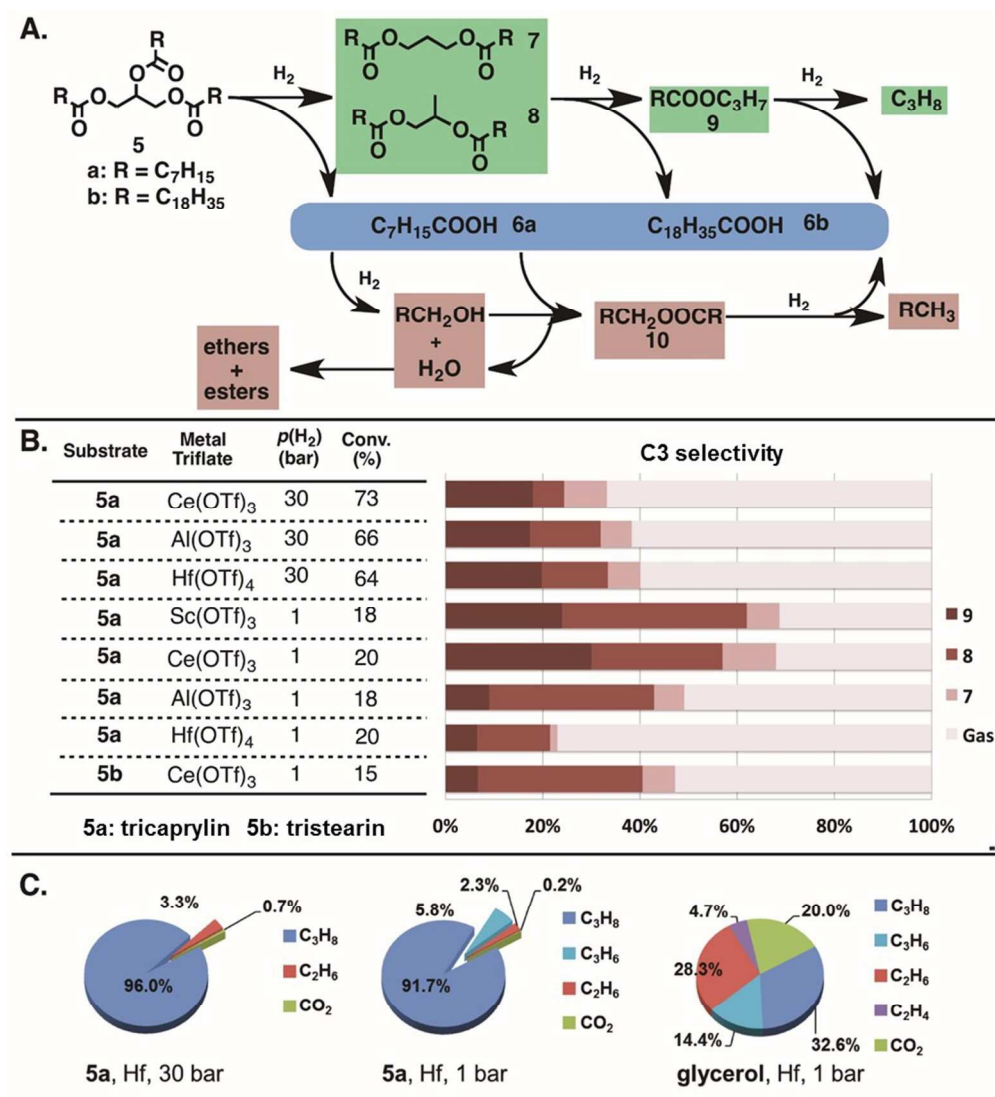
1960x1314mm (72 x 72 DPI)

167x115mm (150 x 150 DPI)

70x25mm (300 x 300 DPI)

174x190mm (150 x 150 DPI)